Signals of the QCD axion with mass of 17 MeV/c^2: Nuclear transitions and light meson decays

Daniele S. M. Alves*

Theoretical Division, Los Alamos National Laboratory, Los Alamos, New Mexico 87545, USA

(Received 3 November 2020; accepted 11 February 2021; published 23 March 2021; corrected 30 March 2021)

The QCD axion remains experimentally viable in the mass range of $\mathcal{O}(10\ \mathrm{MeV})$ if (i) it couples predominantly to the first generation of SM fermions; (ii) it decays to e^+e^- with a short lifetime $\tau_a \lesssim 4 \times 10^{-14}$ s; and (iii) it has suppressed isovector couplings, i.e., if it is *piophobic*. Remarkably, these are precisely the properties required to explain recently observed anomalies in nuclear deexcitations, *to wit*: the e^+e^- emission spectra of *isoscalar magnetic* transitions of ^{8}Be and ^{4}He nuclei showed a "bumplike" feature peaked at $m_{e^+e^-} \sim 17$ MeV. In this paper, we argue that on-shell emission of the QCD axion (with the aforementioned properties) provides an extremely well-motivated, compatible explanation for the observed excesses in these nuclear deexcitations. The absence of anomalous features in other measured transitions is also naturally explained: *piophobic* axion emission is strongly suppressed in isovector magnetic transitions and forbidden in electric transitions. This QCD axion hypothesis is further corroborated by an independent observation: a $\sim$2–3σ deviation in the measurement of $\Gamma(\pi^0 \to e^+e^-)$ from the Standard Model theoretical expectation. This paper also includes detailed estimations of various axionic signatures in rare light meson decays, which take into account contributions from low-lying QCD resonance exchange, and, in the case of rare kaon decays, the possible effective implementations of $\Delta S = 1$ octet enhancement in chiral perturbation theory. These inherent uncertainties of the effective description of the strong interactions at low energies result in large variations in the predictions for hadronic signals of the QCD axion; in spite of this, the estimated ranges for rare meson decay rates obtained here can be probed in the near future in η/η' and kaon factories.

DOI: 10.1103/PhysRevD.103.055018

I. INTRODUCTION

The past decade has seen a resurgence of interest in the phenomenology of new light particles with feeble interactions with the Standard Model (SM) [1–3]. Motivations have been varied, spurred from the growing belief that dark matter might be part of a more complex *dark sector* with additional matter and force carriers [4–8], but also because light dark sectors could be parasitically explored in the broader U.S. and worldwide neutrino program [9–12]. Experimental signatures of dark sectors are being searched for by a diverse suite of experiments ranging from beam dumps/fixed targets to meson factories.[1] This effort drew on the legacy of an earlier, very active period of "intensity frontier" experiments initiated in the 1970s. This earlier period, however, was driven partly by studies of hadronic and neutrino physics, and partly by searches for the Higgs boson and the QCD axion. Indeed, in its original incarnation, the QCD axion was part of the electroweak Higgs sector and had its mass spanning the range of $\mathcal{O}(100\ \mathrm{keV}$–$1\ \mathrm{MeV})$ [14–17]. With increasing constraints and no discoveries, laboratory searches for the QCD axion withered away in the early 1990s. By then, the consensus was that the Peccei-Quinn (PQ) mechanism had to take place at much higher energy scales, resulting in the "invisible" axion [18–20]. The tradeoff for foregoing PQ symmetry breaking at the electroweak scale was an ultralight axion with the correct cosmological relic abundance to explain dark matter [21–23], which has been the focus of several ongoing and proposed experiments [24–35].

Nonetheless, motivations for the scale of PQ symmetry breaking are a matter of theoretical prejudice. In the original PQWW (Peccei-Quinn-Weinberg-Wilczek) axion model, a single mechanism to break PQ and electroweak symmetries tackled two major puzzles at once—the absence of CP violation in the strong interactions and

*spier@lanl.gov

[1]See, e.g., talks at the kickoff meeting of the RF6 SNOWMASS Working Group, *"Dark Sectors at High Intensities,"* August 12–13, 2020, [13].

the generation of masses for SM particles.[2] Conversely, axion models with high PQ breaking scales $f_{\rm PQ} \gtrsim 10^9$ GeV could simultaneously address the strong CP problem and the origin of dark matter. In this paper, we focus on yet another possibility, whereby the PQ mechanism is realized by new dynamics close to the QCD scale. Considering that the solution to the strong CP problem provided by the PQ mechanism is intimately connected with the nonperturbative dynamics of QCD, it is not farfetched to suppose that their scales should not be separated by over 10 orders of magnitude. Indeed, such wide separation of scales makes the delicate cancellation mechanism of the strong CP phase vulnerable to spoiling effects, such as nonperturbative quantum gravity effects, which, based on general arguments, are expected to violate global symmetries [37–41] (see also [42] for a shared point of view). Furthermore, existing anomalies in nuclear transitions [43,44] and in the π^0 decay width to e^+e^- [45], if confirmed as beyond the Standard Model (BSM) phenomena, would strongly support the possibility of a low PQ scale axion, as we shall discuss.

A light BSM sector realizing the PQ mechanism at a scale of $\mathcal{O}(\text{GeV})$ cannot be completely generic, however. Any new degrees of freedom must either have weak or nongeneric couplings to avoid existing experimental constraints (which is the case of the *electrophilic*, *muophobic*, and *piophobic* QCD axion studied in [46]), or they must have predominantly hadronic couplings and "blend in" with the QCD resonances in the spectral range of ∼400 MeV–2 GeV. The phenomenology of the latter is quite challenging to predict and to probe experimentally. On the other hand, the inevitable pseudo-Goldstone degree of freedom, manifested as the QCD axion, is much more amenable to phenomenological studies using Chiral Perturbation Theory (χPT). Indeed, a robust prediction of χPT is that the mass of the QCD axion should lie in the range $m_a \sim 1$–20 MeV when its decay constant is $f_a \sim \mathcal{O}(1$–$10)$ GeV. For generic models in this range, the axion mixing angle with the neutral pion is quite large, $\theta_{a\pi} \sim \mathcal{O}(f_\pi/f_a) \sim \mathcal{O}(0.01$–$0.1)$, and strongly excluded by bounds on rare pion decays, which require $\theta_{a\pi} \lesssim \mathcal{O}(10^{-4})$. However, as shown in [46], axion-pion mixing can be suppressed well below its generic magnitude if the axion couples exclusively with light quarks, u and d, with PQ-charge assignments $q^u_{\rm PQ} = 2q^d_{\rm PQ}$. In this special region of parameter space, the phenomenology of the QCD axion is no longer dominated by its isovector couplings; instead, it is largely determined by its isoscalar mixings with the η and η' mesons. As such, it inherits the same strong dependence of the η and η' on higher order terms in the chiral expansion, and its hadronic couplings suffer from $\mathcal{O}(1)$ uncertainties.

Despite these large uncertainties stemming from χPT, it is still possible to parametrize the dependence of a variety of hadronic signatures of the axion in terms of its isovector and isoscalar mixing angles, while remaining agnostic about their magnitudes. The usefulness of such parametrization is manifest when confronting experimental data, not only in constraining the axion's hadronic mixing angles, but also in interpreting experimental anomalies as potential signals of the QCD axion. This will be the underlying philosophy of this study.[3]

Complementary, the underlying motivation for this study is a combination of the long-standing puzzle posed by the strong CP problem, and three independent experimental anomalies. The first two refer to bumplike excesses observed in specific magnetic transitions of ^{8}Be and ^{4}He nuclei via e^+e^- emission, with (naïve) significances of 6.8σ [43] and 7.2σ [44], respectively. The third anomaly is related to the persistently high central value observed for the width $\Gamma(\pi^0 \to e^+e^-)$, whose most recent and precise measurement, performed by the KTeV Collaboration in 2007 [45], showed a discrepancy from the theoretical expectation in the SM at the level of ∼2–3.2σ [48–51]. In combination, these anomalies point to a common BSM origin: a new short-lived boson with mass of ∼16–17 MeV, coupled to light quarks and electrons, and decaying predominantly to e^+e^- (see also [52] for connections with other anomalies). As an *ad hoc* explanation, there are only two possibilities for the spin and parity of this hypothetical new boson: it can either be a pseudoscalar ($J^P = 0^-$), or an axial vector ($J^P = 1^+$), in order to simultaneously account for these three excesses.[4] Further constraints push these two possibilities into peculiar regions of parameter space, which may require contrived and/or baroque UV completions.[5] At face value, neither of them is particularly compelling, leading many to believe that these

[2]Amusingly, the original axion was allegedly nicknamed *higglet* by Roberto Peccei and Helen Quinn. *Higglet* was also the terminology used by Bill Bardeen and Henry Tye in [36].

[3]This same philosophy was adopted by the authors of [47] in the study of hadronically coupled axionlike particles (ALPs).

[4]In particular, the 1^- *protophobic* vector boson proposed by Feng *et al.* in [53,54] as an explanation of the ^{8}Be anomaly cannot be emitted in the $0^- \to 0^+$ transition of ^{4}He, nor does it contribute non-negligibly to $\Gamma(\pi^0 \to e^+e^-)$. In [55], Feng *et al.* proposed an alternative explanation of the ^{4}He anomaly, whereby the e^+e^- excess stems from the deexcitation of the overlapping 0^+ nuclear state. Recently, [56] argued that the protophobic vector boson hypothesis is excluded as an explanation of the ^{8}Be anomaly.

[5]For instance, in the axial-vector case, the model building required to circumvent stringent bounds from electron-neutrino scattering restricts the axial-vector couplings of the 1^+ state to light quarks to satisfy $g^A_u = -2g^A_d$ [57,58]; axial-vector models also typically require many *ad hoc* degrees of freedom to cancel gauge anomalies in the UV. In the axion case, in order to suppress $a - \pi^0$ mixing, the PQ charges of the up and down quarks must satisfy $q^u_{\rm PQ} = 2q^d_{\rm PQ}$, with (nearly) vanishing PQ charges for the other quarks. Such flavor alignment, combined with the fact that $f_{\rm PQ} \sim \mathcal{O}(\text{GeV})$, requires nontrivial UV completion at the weak scale; see [46].

anomalies are either the result of experimental systematics and/or poorly understood SM effects. In our opinion, this illustrates the paradoxical predicament of the light dark sector intensity frontier program: the generic models it seeks to discover or rule out are not strongly motivated, and, at least historically, it has been the case that experimental excesses without theoretically compelling interpretations tend to be received with strong skepticism.

Fortunately, this predicament might not be warranted here. Nuclear transitions via axion emission and (modified) rare meson decays are smoking gun signatures of the QCD axion which have been predicted over three decades ago [59–66]. The fact that some of these signatures have appeared in ^{8}Be, ^{4}He, and π^0 decays, and can be consistently explained by a QCD axion variant which remains experimentally viable (albeit with peculiar properties of electrophilia, muophobia, and piophobia), should be taken with cautious optimism.

After a brief overview of the most relevant properties of the piophobic QCD axion in Sec. II, we obtain the parameter space of axion isoscalar couplings favored by the ^{8}Be and ^{4}He anomalies, and, taking into account nuclear and hadronic uncertainties, show that they significantly overlap, favoring the QCD axion emission hypothesis as a single explanation of both anomalies (Sec. III). We then turn to axion signals in rare meson decays. In Sec. IV A, we obtain the parametric dependence of η/η' dielectronic decays on the axion's isoscalar mixing angles. In Sec. IV B, we calculate the rate for axio-hadronic decays of the η and η' mesons in the framework of *Resonance Chiral Theory*, an effective "UV completion" of χPT that incorporates low-lying QCD resonances and extends the principle of *Vector Meson Dominance*. Finally, in Sec. V, we investigate various axionic decays of charged and neutral kaons, considering distinct possible implementations of octet enhancement in χPT and their effect on axionic kaon decay rates. We conclude in Sec. VI.

II. BRIEF OVERVIEW OF THE PIOPHOBIC QCD AXION

Generic models of the QCD axion with mass of ∼16–17 MeV are largely excluded. However, as investigated in [46], all experimental constraints to date can be avoided in this mass range if the axion satisfies a few specific requirements which are as follows:

(i) It must be short lived ($\tau_a \lesssim 0.4 \times 10^{-13}$ s) and decay predominantly to e^+e^- in order to avoid limits from beam dump and fixed target experiments, as well as constraints from charged kaon decays such as $K^+ \to \pi^+(a \to \gamma\gamma, \text{invisible})$.

(ii) The PQ charges of second and third generation SM fermions must vanish or be suppressed, in order to avoid limits from the muon anomalous magnetic dipole moment, $(g-2)_\mu$, and from upper bounds on radiative quarkonium decays: $J/\Psi, \Upsilon \to \gamma(a \to e^+e^-)$.

(iii) The $a-\pi^0$ mixing must be suppressed, $\theta_{a\pi} \lesssim \mathcal{O}(10^{-4})$, in order to respect upper bounds on $\text{Br}(\pi^+ \to e^+\nu_e(a \to e^+e^-))$.

A simple phenomenological IR model realizing the requirements above can be easily incorporated in the post-electroweak symmetry breaking SM Lagrangian by ascribing axionic phases to the masses of the up-quark, down-quark, and electron,

$$\begin{aligned} m_u &\to m_u e^{i\gamma^5 q^u_{\rm PQ} a/f_a}, \\ m_d &\to m_d e^{i\gamma^5 q^d_{\rm PQ} a/f_a}, \\ m_e &\to m_e e^{i\gamma^5 q^e_{\rm PQ} a/f_a}, \end{aligned} \tag{1}$$

where $q^f_{\rm PQ}$ ($f = u, d, e$) are PQ charges, with $q^e_{\rm PQ} \sim \mathcal{O}(1)$ and $q^u_{\rm PQ} = 2q^d_{\rm PQ}$. Importantly, no additional operators should be present in this specific basis, such as derivative couplings of the axion to quark axial currents, or the usual linear coupling of the axion to the gluon dual field strength operator.

In this IR model, requirement (ii) mentioned above has been imposed by *fiat*. Requirement (i) follows from the axion's coupling to e^+e^-, which dominates its decay width,

$$\Gamma(a \to e^+e^-) = \frac{m_a}{8\pi}\left(\frac{q^e_{\rm PQ} m_e}{f_a}\right)^2 \sqrt{1-\frac{4m_e^2}{m_a^2}}, \tag{2}$$

$$\Rightarrow \tau_a \approx \frac{4\times 10^{-15}\ \text{s}}{(q^e_{\rm PQ})^2}. \tag{3}$$

For $m_a \sim 16$–17 MeV, existing bounds on the electron's PQ charge are very mild, limiting its range to $1/3 \lesssim |q^e_{\rm PQ}| \lesssim 2$. The upper bound is set by KLOE's 2015 search for visibly decaying dark photons [67], whereas the lower bound is set by the 2019 results from CERN's SPS NA64 fixed target experiment [68,69], constraining the axion lifetime to $\tau_a \lesssim 0.4 \times 10^{-13}$ s. The sensitivities of future experiments to the axion's electronic couplings (such as fixed targets and e^+e^- colliders) have been explored in [46].

From (1) and standard χPT at leading order, the axion mass is given by

$$m_a = \frac{|q^u_{\rm PQ} + q^d_{\rm PQ}|}{\sqrt{1+\epsilon_s}} \frac{\sqrt{m_u m_d}}{(m_u+m_d)} \frac{m_\pi f_\pi}{f_a}, \tag{4}$$

with

$$\epsilon_s \approx \frac{m_u m_d}{(m_u+m_d)^2}\frac{m_\pi^2}{m_K^2}\left(1+6\frac{m_K^2}{m_{\eta'}^2}\right) \simeq 0.04. \tag{5}$$

It follows then that for $q^u_{\rm PQ}/2 = q^d_{\rm PQ} = 1$ and $m_a = 16.7$ MeV, the axion decay constant is $f_a \simeq 1030$ MeV.

We will benchmark m_a, f_a, $q^u_{\rm PQ}$, and $q^d_{\rm PQ}$ to these values for the remainder of this paper.

For generic parameter space of QCD axion models, the quark mass hierarchy $m_{u,d} \ll m_s$ typically induces a hierarchy of axion-meson mixing angles, $\theta_{a\pi} \gg \theta_{a\eta}, \theta_{a\eta'}$, resulting in the isovector couplings of the axion dominating its experimental signatures. This is not the case for the piophobic axion we are considering. Here, the $a-\pi^0$ mixing angle, to leading order in χPT, is given by

$$\theta_{a\pi}|_{\chi\rm PT\,LO} = -\frac{f_\pi}{f_a}\left(\frac{(m_u q^u_{\rm PQ} - m_d q^d_{\rm PQ})}{m_u+m_d} + \epsilon_s \frac{(q^u_{\rm PQ} - q^d_{\rm PQ})}{2}\right)\frac{1}{1+\epsilon_s}, \tag{6}$$

which, after taking $q^u_{\rm PQ}/2 = q^d_{\rm PQ} = 1$ and $m_u/m_d = 0.485 \pm 0.027$ from [70], results in

$$\theta_{a\pi}|_{\chi\rm PT\,LO} = (-0.02 \pm 3)\times 10^{-3}. \tag{7}$$

It is clear from (6) and (7) that the axion's *piophobia* is the result of an accidental cancellation in χPT's leading order contribution to $\theta_{a\pi}$. This cancellation stems from the near numerical coincidence between m_u/m_d and $q^d_{\rm PQ}/q^u_{\rm PQ} = 1/2$.

Unfortunately, χPT's prediction (7) alone is not precise enough to be useful. We instead have resort to observation to determine the allowed range for $\theta_{a\pi}$ with better precision. This can be achieved by requiring that the 3.2σ excess in KTeV's measurement of $\Gamma(\pi^0 \to e^+e^-)$ [45] be the result of $\pi^0 - a$ mixing, which yields [46]

$$\theta_{a\pi}|_{\rm KTeV} = \frac{(-0.6 \pm 0.2)}{q^e_{\rm PQ}}\times 10^{-4}. \tag{8}$$

Given the suppressed value (8) for $\theta_{a\pi}$, this model features an atypical hierarchy of mixing angles, $\theta_{a\pi} \ll \theta_{a\eta}, \theta_{a\eta'}$, which results in the isoscalar couplings of the axion dominating its experimental signatures. This aggravates the loss of χPT's usual predictive power in axion phenomenology—given its state of the art, χPT cannot numerically pin down the isoscalar mixing angles $\theta_{a\eta}$, $\theta_{a\eta'}$ with good accuracy. As argued in [46], $\theta_{a\eta}$, $\theta_{a\eta'}$ receive $\mathcal{O}(1)$ contributions from operators at $\mathcal{O}(p^4)$ in the chiral expansion, many of which have poorly determined Wilson coefficients.

Any substantive theoretical progress in better determining the axion's hadronic couplings is unlikely to be accomplished anytime soon. Indeed, such efforts might be superseded by future experimental results which will be able to either exclude or narrow down the preferred ranges for the axion's isoscalar couplings. With this in mind, in this study we choose to remain agnostic about their magnitude and instead simply parametrize the *physical* axion current as[6]

$$J^{a_{\rm phys}}_\mu \equiv f_a \partial_\mu a_{\rm phys} \equiv \frac{f_a}{f_\pi}(f_\pi \partial_\mu a + \theta_{a\pi} J^{(3)}_{5\mu} + \theta_{a\eta_{ud}} J^{(ud)}_{5\mu} + \theta_{a\eta_s} J^{(s)}_{5\mu}), \tag{9}$$

where

$$J^{(3)}_{5\mu} \equiv \frac{\bar u \gamma_\mu\gamma_5 u - \bar d\gamma_\mu\gamma_5 d}{2} \equiv f_\pi \partial_\mu \pi_3, \tag{10a}$$

$$J^{(ud)}_{5\mu} \equiv \frac{\bar u \gamma_\mu\gamma_5 u + \bar d\gamma_\mu\gamma_5 d}{2} \equiv f_\pi \partial_\mu \eta_{ud}, \tag{10b}$$

$$J^{(s)}_{5\mu} \equiv \frac{\bar s \gamma_\mu\gamma_5 s}{\sqrt{2}} \equiv f_\pi \partial_\mu \eta_s. \tag{10c}$$

The axionic field a and the neutral meson degrees of freedom π_3, η_{ud}, and η_s in (10) mix among themselves to yield the physical degrees of freedom (i.e., the mass eigenstates) $a_{\rm phys}$, π^0, η, and η'. In particular, the implication of (9) is that any strong or weak process involving the currents in (10) will have a corresponding axion signature for which one of the neutral mesons in the amplitude gets replaced by $a_{\rm phys}$ properly weighted by the appropriate mixing angle.

With the parametrization in (9), it is straightforward to obtain the axion's couplings to photons and nucleons. Specifically, below the QCD confinement scale, the electromagnetic anomaly of the physical axion current (9) leads to

$$\mathcal{L}_a \supset \frac{\alpha}{4\pi f_\pi}\left(\theta_{a\pi} + \frac{5}{3}\theta_{a\eta_{ud}} + \frac{\sqrt{2}}{3}\theta_{a\eta_s}\right) a F_{\mu\nu}\tilde F^{\mu\nu}, \tag{11}$$

which, combined with (2), yields the axion decay width and branching ratio to two photons,

$$\Gamma(a\to\gamma\gamma) = \left(\theta_{a\pi} + \frac{5}{3}\theta_{a\eta_{ud}} + \frac{\sqrt{2}}{3}\theta_{a\eta_s}\right)^2 \left(\frac{\alpha}{4\pi f_\pi}\right)^2 \frac{m_a^3}{4\pi}, \tag{12}$$

$$\Rightarrow {\rm Br}(a\to\gamma\gamma) \approx 10^{-7}\times \frac{1}{(q^e_{\rm PQ})^2}\left(\frac{\theta_{a\pi} + \frac{5}{3}\theta_{a\eta_{ud}} + \frac{\sqrt{2}}{3}\theta_{a\eta_s}}{10^{-3}}\right)^2. \tag{13}$$

The axion's contribution to $(g-2)_e$ stemming from its couplings to electrons and photons has been worked out in [46].

[6]We omit the dependence of (9) on $\bar e\gamma_\mu\gamma_5 e$, which has no bearing on the axion-meson mixing angles.

Finally, expressing the axion nuclear couplings generically as

$$\mathcal{L}_{aNN} = a\bar{N}i\gamma^5(g^{(0)}_{aNN} + g^{(1)}_{aNN}\tau^3)N, \tag{14}$$

the parametrization in (9) yields the following isovector and isoscalar axion-nucleon couplings, respectively:

$$g^{(1)}_{aNN} = \theta_{a\pi}g_{\pi NN} = \theta_{a\pi}(\Delta u - \Delta d)\frac{m_N}{f_\pi}, \tag{15a}$$

$$g^{(0)}_{aNN} = (\theta_{a\eta_{ud}}(\Delta u + \Delta d) + \sqrt{2}\theta_{a\eta_s}\Delta s)\frac{m_N}{f_\pi}. \tag{15b}$$

Above, N is the nucleon isospin doublet, m_N is the nucleon mass, and Δq quantifies the matrix elements of quark axial-currents in the nucleon via $2s_\mu\Delta q = \langle N|\bar{q}\gamma_\mu\gamma_5 q|N\rangle$, with s_μ the nucleon spin vector. The combination in (15a) is well determined from neutron β decay,

$$\Delta u - \Delta d = g_A \simeq 1.27. \tag{16}$$

On the other hand, estimations for $\Delta u + \Delta d$ and Δs based on data from semileptonic hyperon decays, proton deep inelastic scattering, and lattice calculations vary widely [71–83], ranging from

$$0.09 \lesssim \Delta u + \Delta d \lesssim 0.62 \quad \text{and} \quad -0.35 \lesssim \Delta s \lesssim 0. \tag{17}$$

In the following, we will use (15) to fit the recent ^{8}Be and ^{4}He anomalies, and (9) to obtain various rare meson decays.

III. NUCLEAR TRANSITIONS

One of the smoking gun signatures of axions in the mass range $\mathcal{O}$(keV–MeV) are magnetic nuclear deexcitations via axion emission [59–61]. Indeed, such signals have been extensively searched for during the 1980s [84–93]. However, since the energy of typical nuclear transitions ranges from a few keV to a few MeV, past searches did not place meaningful bounds on axions heavier than $m_a \gtrsim 2$ MeV.

Recently, the MTA Atomki Collaboration led by A. Krasznahorkay reported on the observation of bumplike excesses in the invariant mass distribution of e^+e^- pairs emitted in the deexcitation of specific states of ^{8}Be and ^{4}He nuclei [43,44]. The energy difference ΔE between the nuclear levels involved in these particular transitions is atypically high, *a priori* allowing on-shell emission of particles as heavy as ∼17–18 MeV. Furthermore, consistent with the allowed values of angular momentum and parity carried away by the axion ($J^P = 0^-, 1^+, 2^-, 3^+, \ldots$), these excesses appeared in *magnetic* (but not *electric*) transitions. Also, consistent with the emission of a piophobic axion, these excesses were observed only in predominantly *isoscalar* (but not *isovector*) transitions. Axion emission rates for the magnetic dipole transitions of ^{8}Be have already been worked out in [46]; we briefly review the main results here to make this section self-contained. We then estimate the expected axion emission rate for the magnetic monopole transition of ^{4}He investigated by Krasznahorkay *et al.* and show that the reported excess rates for both nuclei favor the same range of axion isoscalar mixing angles.

A. Evidence for the QCD axion in ^{8}Be transitions

In [43], the MTA Atomki experiment selectively populated specific excited states of the ^{8}Be nucleus by impinging a beam of protons with finely tuned energy on a ^{7}Li target. They then measured the energy and angular correlation of e^+e^- pairs emitted in deexcitations of these states to the ground state of ^{8}Be. From these measurements, they were able to reconstruct final state kinematic variables, such as the invariant mass of the e^+e^- pair, $m_{e^+e^-}$. The nuclear levels of interest deexcited to the ground state via magnetic dipole (M1) transitions,

$$^8\text{Be}^*(17.64) \to {}^8\text{Be}(0) + e^+e^-, \qquad \Delta E = 17.64\ \text{MeV}, \quad \Delta I \approx 1, \tag{18a}$$

$$^8\text{Be}^*(18.15) \to {}^8\text{Be}(0) + e^+e^-, \qquad \Delta E = 18.15\ \text{MeV}, \quad \Delta I \approx 0. \tag{18b}$$

Above, ^{8}Be(0) is the $J^P = 0^+$ isospin-singlet ground state of the ^{8}Be nucleus, and ^{8}Be*(17.64) and ^{8}Be*(18.15) are $J^P = 1^+$ excited states, whose isospin quantum numbers are predominantly $I = 1$ and $I = 0$, respectively, but are nonetheless isospin mixed,

$$|^8\text{Be}^*(17.64)\rangle = \sin\theta_{1^+}|I = 0\rangle + \cos\theta_{1^+}|I = 1\rangle, \tag{19a}$$

$$|^8\text{Be}^*(18.15)\rangle = \cos\theta_{1^+}|I = 0\rangle - \sin\theta_{1^+}|I = 1\rangle. \tag{19b}$$

Their level of isospin mixing, quantified by θ_{1^+}, was estimated by *ab initio* quantum Monte Carlo techniques [54,94] and by χEFT many-body methods [58] to fall in the approximate range $0.18 \lesssim \sin\theta_{1^+} \lesssim 0.43$. Following [54,58], we will consider a narrower range for $\sin\theta_{1^+}$ which more accurately describes the width of the electromagnetic transition $^8\text{Be}^*(18.15) \to {}^8\text{Be}(0) + \gamma$,

$$0.30 \leq \sin\theta_{1^+} \leq 0.35. \tag{20}$$

In the MTA Atomki experiment [43], a bumplike feature in the $m_{e^+e^-}$ distribution of the $\Delta I \approx 0$ transition (18b) was observed on top of the monotonically falling spectrum expected from SM internal pair conversion (IPC) [43]. A statistical significance of 6.8σ was reported for this deviation relative to the IPC expectation. Additionally, it was claimed in [43] that the excess events were consistent with the

emission of an on-shell resonance, generically labeled "X," with mass of $m_X = (16.7 \pm 0.35_{\rm stat} \pm 0.5_{\rm syst})\,{\rm MeV}$, promptly decaying to e^+e^-. This excess was later corroborated by the same collaboration with a modified experimental setup [95], with a combined fit yielding a relative branching ratio of

$$\left.\frac{\Gamma_X}{\Gamma_\gamma}\right|_{^8{\rm Be}^*(18.15)} \approx (6 \pm 1) \times 10^{-6}, \tag{21}$$

with respect to the radiative γ width of this transition, $^8{\rm Be}^*(18.15) \to {}^8{\rm Be}(0) + \gamma$, of $\Gamma_\gamma(18.15) \approx (1.9 \pm 0.4)\,{\rm eV}$ [96].

As for the $m_{e^+e^-}$ spectrum of the $\Delta I \approx 1$ transition (18a), no statistically significant deviation from the IPC expectation was observed. References [53,58] inferred a naïve upper bound of

$$\left.\frac{\Gamma_X}{\Gamma_\gamma}\right|_{^8{\rm Be}^*(17.64)} \lesssim \mathcal{O}(10^{-6}) \tag{22}$$

for the deexcitation rate of $^8{\rm Be}^*(17.64)$ via on-shell emission of this hypothetical "$X(17)$" resonance.

If it is confirmed that the observed excess originates from new, beyond the SM phenomena, as opposed to nuclear physics effects or experimental systematics, it could indeed be explained by the piophobic QCD axion. The prediction for axion emission rates from magnetic dipole nuclear transitions was first worked out by Treiman and Wilczek [59] and independently by Donnelly *et al.* [60] back in the late 1970s. For the two transitions in (18), the axion-to-photon emission rate is (see also [61,63,90])

$$\left.\frac{\Gamma_a}{\Gamma_\gamma}\right|_{^8{\rm Be}^*} = \frac{1}{2\pi\alpha}\left|\frac{\sum_{I=0,1} g_{aNN}^{(I)} \langle I|^8{\rm Be}^*\rangle}{\sum_{I=0,1}(\mu^{(I)} - \eta^{(I)})\langle I|^8{\rm Be}^*\rangle}\right|^2 \left(1 - \frac{m_a^2}{\Delta E^2}\right)^{3/2}, \tag{23}$$

where $|^8{\rm Be}^*\rangle$ denotes one of the states in (18), and its overlap with the isospin eigenstates $|I=0\rangle$ and $|I=1\rangle$ follows from (19). The quantities $\mu^{(0)} = \mu_p + \mu_n = 0.88$ and $\mu^{(1)} = \mu_p - \mu_n = 4.71$ are, respectively, the isoscalar and isovector nuclear magnetic moments, and $\eta^{(0)}$, $\eta^{(1)}$ parametrize ratios of nuclear matrix elements of convection and magnetization currents [89]. In particular, $\eta^{(0)} = 1/2$ due to total angular momentum conservation. The nuclear structure dependent parameter $\eta^{(1)}$, to the best of our knowledge, has not been calculated for ^{8}Be; we therefore conservatively vary $\eta^{(1)}$ in the range

$$-1 \le \eta^{(1)}|_{^8{\rm Be}} \le 1. \tag{24}$$

Combining (23) with (15), (16), (18b), and (19b), we can infer the axion isoscalar mixing angles that yield the observed excess rate (21). For concreteness, we vary $\theta_{a\pi}$ within the 1σ range favored by the KTeV anomaly fit, (8), while also varying $q^e_{\rm PQ}$ in the range $1/2 \le q^e_{\rm PQ} \le 2$, and the nuclear structure parameters θ_{1^+} and $\eta^{(1)}$ in the ranges (20) and (24), respectively. We obtain

$$-(\theta_{a\eta_{ud}}(\Delta u + \Delta d) + \sqrt{2}\theta_{a\eta_s}\Delta s)|_{^8{\rm Be}^*(18.15)} \approx (1.1\text{–}6.3) \times 10^{-4}. \tag{25}$$

Figure 1 displays the parameter space in $\theta_{a\eta_{ud}}$ versus $\theta_{a\eta_s}$ favored by the ^{8}Be anomaly (orange bands) under the assumptions of $\Delta u + \Delta d = 0.52$, $\Delta s = -0.022$ [97], and equal (upper plot) or opposite (lower plot) relative sign

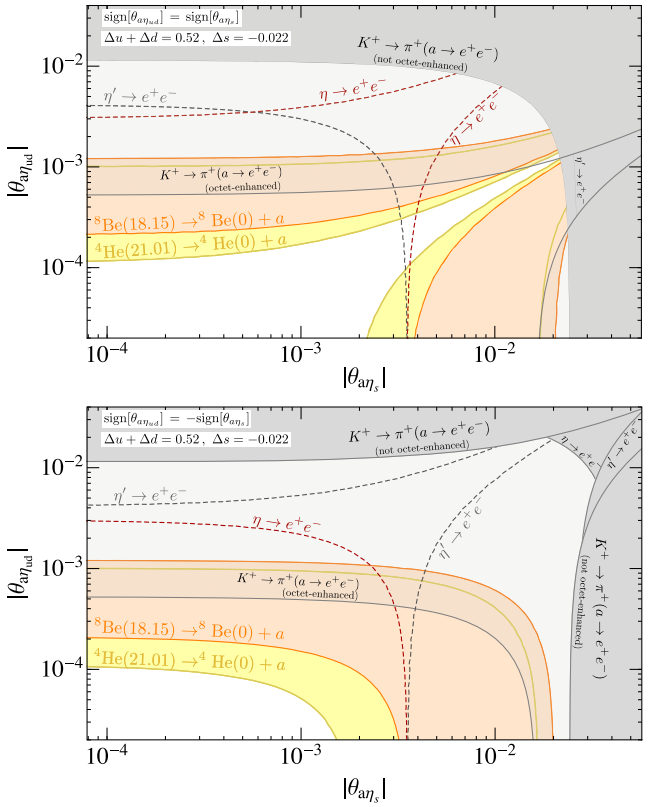

FIG. 1. Fits, constraints, and sensitivity projections in the parameter space of the axion isoscalar couplings. The upper (lower) plot assumes the same (opposite) relative sign between $\theta_{a\eta_{ud}}$ and $\theta_{a\eta_s}$. The orange and yellow bands enclose the range of isoscalar mixing angles that can explain the ^{8}Be and ^{4}He anomalies, respectively, benchmarking $\Delta u + \Delta d$ and Δs to the values shown; cf. (25), (33). The shaded gray regions are excluded by the conservative upper bound ${\rm Br}(K^+ \to \pi^+(a \to e^+e^-)) \lesssim 10^{-5}$ (under different scenarios for octet enhancement in χPT) and by current bounds on $\eta^{(\prime)} \to e^+e^-$, assuming $q^e_{\rm PQ} = 1/2$; cf. (34a) and (35a). The dashed gray (red) lines show the expected reach from measurements of (or bounds on) $\eta'(\eta) \to e^+e^-$, assuming that future experiments will have sensitivity to the branching ratios predicted in the SM, (34b) and (35b), with $\mathcal{O}(1)$ precision.

between $\theta_{a\eta_{ud}}$ and $\theta_{a\eta_s}$. These bands shift non-negligibly as $\Delta u + \Delta d$ and Δs are varied within the ranges in (17).

Finally, we conclude this discussion by using (23) and (25) to predict the axion emission rate for transition (18a)

$$\left.\frac{\Gamma_a}{\Gamma_\gamma}\right|_{^8\mathrm{Be}^*(17.64)} \approx (0.008\text{–}1) \times 10^{-6}. \tag{26}$$

Indeed, this rate can be down by as much as 2 orders of magnitude below the sensitivity of published results to date, but could potentially be detectable if sufficient statistics is accumulated in this channel.

B. Evidence for the QCD axion in ^{4}He transitions

More recently, the same collaboration led by A. Krasznahorkay investigated transitions of a different nucleus, ^{4}He [44]. With a 900 keV proton beam bombarding a ^{3}H fixed target, this experiment populated the first two excited states of ^{4}He,

$$^4\mathrm{He}^*(20.49), \quad J^P = 0^+, \quad I = 0, \quad \Gamma = 0.50\,\mathrm{MeV}, \tag{27a}$$

$$^4\mathrm{He}^*(21.01), \quad J^P = 0^-, \quad I = 0, \quad \Gamma = 0.84\,\mathrm{MeV}, \tag{27b}$$

and similarly measured the emission of e^+e^- pairs from deexcitations of these states to the $I = 0$, $J^P = 0^+$ ground state, denoted here by ^{4}He(0). Such transitions are allowed via

$$\text{(E0)} \quad ^4\mathrm{He}^*(20.49) \to {}^4\mathrm{He}(0) + (\gamma^* \to e^+e^-), \quad \Delta E = 20.49\,\mathrm{MeV}, \quad \Delta I = 0, \tag{28a}$$

$$\text{(M0)} \quad ^4\mathrm{He}^*(21.01) \to {}^4\mathrm{He}(0) + (a \to e^+e^-), \quad \Delta E = 21.01\,\mathrm{MeV}, \quad \Delta I = 0, \tag{28b}$$

but *forbidden* to occur via the following processes:

$$\text{(E0)} \quad ^4\mathrm{He}^*(20.49) \not\to {}^4\mathrm{He}(0) + (a \to e^+e^-), \tag{29a}$$

$$\text{(M0)} \quad ^4\mathrm{He}^*(21.01) \not\to {}^4\mathrm{He}(0) + (\gamma^* \to e^+e^-). \tag{29b}$$

Above, E0 and M0 refer, respectively, to the electric monopole ($J^P = 0^+$) and magnetic monopole ($J^P = 0^-$) multipolarities of these transitions.

After cuts, background subtraction, and accounting for contributions to the $m_{e^+e^-}$ spectrum from (28a) and from external pair conversion originating from the radiative proton capture reaction $^3\mathrm{H}(p,\gamma)^4\mathrm{He}$, a suggestive bumplike excess was observed in the final $m_{e^+e^-}$ distribution, with a statistical significance of 7.2σ. Under the assumption that this excess originated from on-shell emission of a narrow resonance from the M0 transition (28b), the fit to the data performed in [44] yielded a favored resonance mass of $m_a = (16.84 \pm 0.16_{\mathrm{stat}} \pm 0.20_{\mathrm{syst}})$ MeV, and deexcitation width,[7]

$$\Gamma|_{^4\mathrm{He}^*(21.01)\to{}^4\mathrm{He}(0)+a} \approx 3.9 \times 10^{-5}\ \mathrm{eV}. \tag{30}$$

It is encouraging that not only the same resonance mass (within error bars) is favored by fits to both the ^{4}He and ^{8}Be excesses, but also that they appear in *magnetic* and (dominantly) *isoscalar* transitions, compatible with the interpretation of piophobic axion emission. To further support this hypothesis, we must obtain the range of axion isoscalar mixing angles compatible with the observed rate. According to Donnelly *et al.* [60], the width of axionic emission in $0^- \to 0^+$ nuclear transitions is estimated to be[8]

$$\Gamma_a|_{\mathrm{M0}} \approx \frac{2}{(2I_{N^*}+1)} \frac{|\vec{p}_a|^5}{m_N^2 Q^2} |a^{(0)}_{\mathrm{M0}}\, g^{(0)}_{aNN} + a^{(1)}_{\mathrm{M0}}\, g^{(1)}_{aNN}|^2, \tag{31}$$

where I_{N^*} is the isospin of the excited nuclear state, $|\vec{p}_a| \approx \sqrt{\Delta E^2 - m_a^2}$ is the magnitude of the axion's spatial-momentum in the rest frame of the decaying nucleus, Q is a typical nuclear momentum transfer (of order the nucleus Fermi momentum, $Q \approx k_F \approx 250$ MeV), and $a^{(0)}_{\mathrm{M0}}$, $a^{(1)}_{\mathrm{M0}}$ involve nuclear matrix elements of magnetization currents, and are of $\mathcal{O}(1)$, unless forbidden by isospin conservation. For an isoscalar transition such as (28b), (31) reduces to

$$\left.\Gamma_a\right|_{\mathrm{M0},\Delta I=0} \approx |a^{(0)}_{\mathrm{M0}}|^2 \frac{2(\Delta E^2 - m_a^2)^{5/2}}{m_N^2 Q^2} |g^{(0)}_{aNN}|^2. \tag{32}$$

Using (32) and (15b), and varying $a^{(0)}_{\mathrm{M0}}$ in the range $1/3 \le |a^{(0)}_{\mathrm{M0}}| \le 3$, we find that the axionic deexcitation width of the M0 transition (28b) in ^{4}He yields the observed rate (30) if

[7] No error bars were provided for (30) in [44].

[8] In [55], the calculated rate for pseudoscalar emission in this $0^- \to 0^+$ transition assumed a nonderivatively coupled pseudoscalar "X" (see the effective operator in Eq. (39) of [55]), resulting in an amplitude with no momentum dependence (Eq. (49) of [55]) and an emission rate scaling as $\Gamma_X \propto |\vec{p}_X|$. Under this assumption, the authors of [55] concluded that the rate of pseudoscalar emission in this transition would be 6 orders of magnitude larger than the experimentally favored rate. We point out that their conclusion hinged on their assumption that the leading effective operator at the nuclear level mediating this transition was a relevant operator of dimension 3. In the case of the QCD axion, this assumption is not valid, since the axion only couples derivatively to nuclear axial currents. For the QCD axion, the leading effective nuclear operator is dimension 5, resulting in an amplitude scaling as $\propto |\vec{p}_a|^2$, and therefore an emission rate scaling as $\Gamma_a \propto |\vec{p}_a|^5$. Note that the axionic amplitude is still isotropic, as it should be for a monopole transition, despite its nontrivial momentum dependence. For details, see [60,61,98].

$$- (\theta_{a\eta_{ud}}(\Delta u + \Delta d) + \sqrt{2}\theta_{a\eta_s}\Delta s)|_{^4\mathrm{He}^*(21.01)} \approx (0.58\text{–}5.3) \times 10^{-4}, \quad (33)$$

which is compatible with the range of axion isoscalar mixing angles favored by the ^{8}Be excess, (25). In Fig. 1, we likewise display the parameter space in $\theta_{a\eta_{ud}}$ versus $\theta_{a\eta_s}$ favored by the ^{4}He anomaly (yellow bands) under the same assumptions for $\Delta u + \Delta d$, Δs and relative sign between $\theta_{a\eta_{ud}}$ and $\theta_{a\eta_s}$ used in the computation of the ^{8}Be orange bands. The ^{4}He yellow bands also shift non-negligibly as $\Delta u + \Delta d$ and Δs are varied within the ranges in (17).

It is remarkable that the piophobic QCD axion is able to *simultaneously* explain the reported rate of anomalous excesses in deexcitations of two very different nuclei, ^{8}Be and ^{4}He, as shown by the overlap between the favored ranges for the axion isoscalar mixing angles (25) and (33), or, equivalently, by the overlap between the yellow and orange bands in Fig. 1. This weakens the case for a nuclear physics origin of the observed features in the $m_{e^+e^-}$ spectra of these transitions [99]. And the fact that "unexplained" features are absent in the $m_{e^+e^-}$ spectrum of several other measured transitions—(18a) being one example—also makes it less straightforward to "explain away" the observed excesses as poorly understood experimental systematics. We therefore reiterate our point, stated in the Introduction (Sec. I), that the anomalies in ^{8}Be and ^{4}He transitions, and their quantitative compatibility with predicted signals from the QCD axion, should not be quickly dismissed. A cautiously optimistic attitude and support for an independent verification of these measurements are certainly warranted, as well as further exploration of other isoscalar magnetic nuclear transitions with $\Delta E \gtrsim 17$ MeV, and radiative $\pi^+/p/n$ capture reactions with significant magnetic components [100].

IV. η AND η' DECAYS

In light of the anomalies in nuclear deexcitations discussed in the previous section, a natural next step is to investigate other systems where the hadronic couplings of the piophobic QCD axion could be more precisely determined or more stringently constrained. In this section, we consider rare decays of η and η' mesons, which, with the prospect of future η/η' factories, could become powerful future probes of axions and hadronically coupled ALPs more generally [101]. These include the second phase of the JLab Eta Factory (JEF) program [102], expected to improve existing bounds on rare η decays by two orders of magnitude, and the REDTOP experiment [103,104], a planned η/η' factory projected to deliver as many as 10^{13} η mesons and 10^{11} η' mesons. These will offer an unprecedented opportunity to study rare η/η' decays and probe BSM physics.

A. Dielectronic η and η' decays

Just as the precise KTeV measurement of $\pi^0 \to e^+e^-$ offered the best determination of $\theta_{a\pi}$, future observations of $\eta \to e^+e^-$ and $\eta' \to e^+e^-$ could narrow down the ranges for the axion isoscalar mixing angles $\theta_{a\eta_{ud}}$ and $\theta_{a\eta_s}$. Present bounds on these dileptonic branching ratios [105,106] are still 2 orders of magnitude away from sensitivity to the predicted SM rate [107–109],

$$\mathrm{Br}(\eta \to e^+e^-)_{\mathrm{exp}} < 7 \times 10^{-7}, \quad (34a)$$

$$\mathrm{Br}(\eta \to e^+e^-)_{\mathrm{SM}} \approx (4.6\text{–}5.4) \times 10^{-9}, \quad (34b)$$

and

$$\mathrm{Br}(\eta' \to e^+e^-)_{\mathrm{exp}} < 0.56 \times 10^{-8}, \quad (35a)$$

$$\mathrm{Br}(\eta' \to e^+e^-)_{\mathrm{SM}} \approx (1\text{–}2) \times 10^{-10}. \quad (35b)$$

Indeed, the highly suppressed SM contribution to these dileptonic channels makes them potentially sensitive to a variety of interesting new physics scenarios.

In anticipation of a future discovery of these decay modes, we obtain the axionic contribution to the dileptonic decays $\eta^{(\prime)} \to e^+e^-$ due to $a - \eta^{(\prime)}$ mixing. Assuming that this effect dominates these rates (i.e., that interference with the SM amplitudes can be neglected), we have

$$\Gamma(\eta^{(\prime)} \to e^+e^-) \approx \frac{m_{\eta^{(\prime)}}}{8\pi}\left(\frac{q^e_{\mathrm{PQ}} m_e}{f_a}\theta_{a\eta^{(\prime)}}\right)^2 \sqrt{1 - \frac{4m_e^2}{m^2_{\eta^{(\prime)}}}}. \quad (36)$$

The mixing angles $\theta_{a\eta}$ and $\theta_{a\eta'}$ can be reexpressed in terms of $\theta_{a\eta_{ud}}$ and $\theta_{a\eta_s}$ using the parametrization [110]

$$|\eta\rangle = \cos\phi_{ud}|\eta_{ud}\rangle - \sin\phi_s|\eta_s\rangle, \quad (37a)$$

$$|\eta'\rangle = \sin\phi_{ud}|\eta_{ud}\rangle + \cos\phi_s|\eta_s\rangle, \quad (37b)$$

from which it follows that (34a) and (35a) translate into relatively weak bounds on the axion isoscalar mixing angles,

$$|\theta_{a\eta}| = |\cos\phi_{ud}\theta_{a\eta_{ud}} - \sin\phi_s\theta_{a\eta_s}| \lesssim \frac{0.014}{|q^e_{\mathrm{PQ}}|}, \quad (38a)$$

$$|\theta_{a\eta'}| = |\sin\phi_{ud}\theta_{a\eta_{ud}} + \cos\phi_s\theta_{a\eta_s}| \lesssim \frac{0.01}{|q^e_{\mathrm{PQ}}|}. \quad (38b)$$

Taking $\phi_{ud} = 39.8°$ and $\phi_s = 41.2°$ from [110] and conservatively assuming $|q^e_{\mathrm{PQ}}| = 1/2$ for concreteness, we display the bounds (38) in Fig. 1.

In Fig. 1, we also show contours of $\theta_{a\eta_{ud}}$ and $\theta_{a\eta_s}$ (dashed lines) for which the axionic contribution to $\eta^{(\prime)} \to e^+e^-$ becomes comparable to that of the SM. These contours can be interpreted as the sensitivity to $\theta_{a\eta_{ud}}$ and $\theta_{a\eta_s}$ in the hypothetical scenario of a future observation of these processes showing an $\mathcal{O}(1)$ deviation from the branching ratios predicted in the SM, (34b) and (35b). It goes without saying that the actual experimental sensitivity of future η/η'-factories to $\theta_{a\eta_{ud}}$ and $\theta_{a\eta_s}$ could be substantially better if $\mathrm{Br}(\eta^{(\prime)} \to e^+e^-)$ could be measured with better than $\mathcal{O}(10\%)$ precision, and if the uncertainties in the SM theoretical predictions could be reduced to the percent level.

B. Axio-hadronic η and η' decays

Hadronic decay channels of η and η' mesons could in principle be hiding promising signals of the QCD axion and/or other hadronically coupled ALPs. Among the most obvious modes are the three-body final states $\eta^{(\prime)} \to \pi^0\pi^0 a, \pi^+\pi^- a$, which have only recently been explored in the literature [47,111]. Indeed, the amplitudes for these processes receive a direct contribution from the leading order potential term in the chiral Lagrangian[9] and could in principle result in considerably large branching ratios. The difficulty with studying hadronic η and η' decays lies in reliably predicting their rates. One of the earliest examples where this difficulty was encountered was in the calculation of $\eta \to 3\pi$, which was significantly underestimated by χPT at leading order [112–115]. Indeed, it has long been understood that contributions from chiral logarithms and strong final state rescattering could not be neglected in the computation of $\eta \to 3\pi$ [116–122]. Similarly, neither the total width nor the Dalitz phase space of $\eta' \to \eta\pi\pi$ is properly described by χPT at $\mathcal{O}(p^2)$ [123,124].

Previous studies [125,126] have shown that such intermediate energy processes can be satisfactorily described by extending χPT to include low-lying meson resonances carrying nonlinear realizations of $SU(3)_\chi$—such as vectors (ρ, ω, K^*, ϕ, …), axial vectors (a_1, f_1, K_1, …), scalars (a_0, f_0, σ, κ, …), and pseudoscalars (η', $\pi(1300)$, …)—and assuming the principle of "resonance dominance" (an extension of vector meson dominance), whereby the low-energy constants (LECs) of the $\mathcal{O}(p^4)$ chiral Lagrangian are saturated by mesonic resonance exchange. This framework, dubbed *Resonance Chiral Theory* (RχT), has been quite successful phenomenologically as an interpolating effective theory between the short-distance QCD description and the low-energy χPT framework, by encoding the most prominent features of nonperturbative strong dynamics [127,128]. There does not appear to be consensus in the literature, however, on which low-lying resonances should be included as degrees of freedom in the RχT Lagrangian, and which resonances should be regarded as dynamically generated poles due to strong S-wave interactions [129,130]. Examples of such "ambiguous" poles include the $\sigma(500)$ and the $\kappa(700)$.

In this subsection, we estimate the rates for $\eta \to \pi\pi a$ and $\eta' \to \pi\pi a$ using RχT. In both cases, we find that the leading order χPT predictions for these decay rates are significantly modified by inclusion of resonance exchange amplitudes. In particular, for $\eta \to \pi\pi a$, there is substantial destructive interference between the leading order amplitude from the $\mathcal{O}(p^2)$ quartic term and the amplitudes generated by tree-level resonance exchange. This is corroborated by performing the same calculation in ordinary χPT at $\mathcal{O}(p^4)$, where one finds that the LECs, in particular L_4, L_5, and L_6, provide $\mathcal{O}(1)$ contributions that destructively interfere with the $\mathcal{O}(p^2)$ amplitude. For $\eta' \to \pi\pi a$, the contributions from resonance exchange (alternatively, from χPT interactions at $\mathcal{O}(p^4)$) are the dominant effect in a significant portion of the parameter space and may enhance this decay rate by an order of magnitude over the leading order χPT prediction. The justification for favoring the RχT framework over $\mathcal{O}(p^4)$-χPT for this calculation is that the former is expected to better capture the Dalitz phase space of the final state, which is relevant when extracting the event acceptance due to momentum cuts in experimental analyses (in particular due to the $e^\pm$ selection criteria). Indeed, we will find that there is strong variation of the amplitude's momentum dependence as we vary the assumptions and parameters of the RχT description, which implies a strong variation in the estimated sensitivity of existing and future experimental analyses. Unfortunately, the variations in these assumptions cannot be narrowed down without further input from experiment. Our main conclusion, therefore, is that one cannot reliably predict neither the total branching ratio, nor the Dalitz phase space, of the decays $\eta^{(\prime)} \to \pi\pi a$. Under reasonable assumptions, our RχT-based estimates vary over 2 orders of magnitude in branching ratio, $\mathrm{Br}(\eta^{(\prime)} \to \pi\pi a) \sim \mathcal{O}(10^{-4}\text{–}10^{-2})$. Nonetheless, this motivates dedicated reanalyses of existing data in final states of $\eta^{(\prime)} \to \pi\pi e^+e^-$, as well as dedicated searches for e^+e^- resonances in these final states in future η/η' factories.

In order to motivate our use of RχT, and also to justify our later approximation of retaining only low-lying *scalar* resonances, we begin by obtaining the main contributions to the amplitude $\mathcal{A}(\eta^{(\prime)} \to \pi^0\pi^0 a)$ in ordinary χPT at $\mathcal{O}(p^4)$. The Lagrangian is [131]

[9]More explicitly, these leading order quartic couplings do not contain derivatives of the axion field, nor do they "descend" from ordinary mesonic quartic terms via axion-meson mixing. Nonetheless, they are still consistent with the axion's pseudo-Goldstone nature because they are proportional to $(\sum_q m_q^{-1})^{-1}$ and therefore vanish in the limit of a massless quark.

$$\begin{aligned}\mathcal{L}_{\chi\mathrm{PT}}|_{\mathcal{O}(p^4)} =& \frac{f_\pi^2}{4}\mathrm{Tr}[D_\mu U^\dagger D^\mu U] + \frac{f_\pi^2}{4}\mathrm{Tr}[2B_0 M_q(a)U + \mathrm{H.c.}] \\ & - \frac{1}{2}M_0^2\eta_0^2 + L_1\mathrm{Tr}[D_\mu U^\dagger D^\mu U]^2 + L_2\mathrm{Tr}[D_\mu U^\dagger D_\nu U]\mathrm{Tr}[D^\mu U^\dagger D^\nu U] \\ & + L_3\mathrm{Tr}[D_\mu U^\dagger D^\mu U D_\nu U^\dagger D^\nu U] + L_4\mathrm{Tr}[D_\mu U^\dagger D^\mu U]\mathrm{Tr}[2B_0 M_q(a)U + \mathrm{H.c.}] \\ & + L_5\mathrm{Tr}[D_\mu U^\dagger D^\mu U(2B_0 M_q(a)U + \mathrm{H.c.})] + L_6\mathrm{Tr}[2B_0 M_q(a)U + \mathrm{H.c.}]^2 \\ & + L_7\mathrm{Tr}[2B_0 M_q(a)U - \mathrm{H.c.}]^2 + L_8\mathrm{Tr}[(2B_0 M_q(a)U)(2B_0 M_q(a)U) + \mathrm{H.c.}] \\ & - iL_9\mathrm{Tr}[F_R^{\mu\nu} D_\mu U D_\nu U^\dagger + F_L^{\mu\nu} D_\mu U^\dagger D_\nu U] + L_{10}\mathrm{Tr}[U^\dagger F_R^{\mu\nu} U F_{L\mu\nu}]. \end{aligned} \tag{39}$$

Above, $f_\pi = 92$ MeV; $\delta^{ij}B_0 = -\langle q^i \bar{q}^j\rangle/f_\pi^2$; M_0 parametrizes the $\mathcal{O}(\mathrm{GeV})$ contribution to the mass of the chiral singlet η_0 from the strong axial anomaly; L_i ($i = 1, \ldots, 10$) are the $\mathcal{O}(p^4)$ χPT LECs [see, e.g., [132] for a review of χPT and definitions of all the terms in (39)]; $M_q(a)$ is the axion-dependent quark mass matrix, transforming as an octet spurion of $SU(3)_\chi$,

$$M_q(a) \equiv \begin{pmatrix} m_u e^{iq_{\mathrm{PQ}}^u a/f_a} & & \\ & m_d e^{iq_{\mathrm{PQ}}^d a/f_a} & \\ & & m_s \end{pmatrix}, \tag{40}$$

and U is the nonlinear representation of the pseudo-Goldstone chiral nonet,

$$\begin{aligned} U &= \mathrm{Exp}\left(i\frac{\sqrt{2}}{f_\pi}\varphi^a\lambda^a\right) \\ \text{with}\quad \varphi^a\lambda^a &\equiv \begin{pmatrix} \frac{\pi^0}{\sqrt{2}} + \frac{\eta_8}{\sqrt{6}} + \frac{\eta_0}{\sqrt{3}} & \pi^+ & K^+ \\ \pi^- & -\frac{\pi^0}{\sqrt{2}} + \frac{\eta_8}{\sqrt{6}} + \frac{\eta_0}{\sqrt{3}} & K^0 \\ K^- & \bar{K}^0 & -\frac{\eta_8}{\sqrt{3/2}} + \frac{\eta_0}{\sqrt{3}} \end{pmatrix}. \end{aligned} \tag{41}$$

Collecting the terms in (39) that provide the dominant contributions to $\mathcal{A}(\eta^{(\prime)} \to \pi^0\pi^0 a)$, we obtain

$$\begin{aligned}\mathcal{L}_{\chi\mathrm{PT}}\Big|_{\mathcal{O}(p^4)} \supset & \frac{\sqrt{1+\hat{L}_4/2}}{1+\hat{L}_6} m_\pi^2 f_\pi^2 (q_{\mathrm{PQ}}^u + q_{\mathrm{PQ}}^d)\frac{m_u m_d}{(m_u+m_d)^2}\left[\hat{\eta}_{ud}\hat{\pi}^2\hat{a}\right. \\ & \left. - \frac{\hat{L}_5}{2(1+\hat{L}_4/2)}\hat{\partial}_\mu\hat{\eta}_{ud}\,\hat{\pi}\,\hat{\partial}^\mu\hat{\pi}\,\hat{a} - \frac{(\hat{L}_5+2\hat{L}_4)}{4(1+\hat{L}_4/2)}\hat{\eta}_{ud}\,\hat{\partial}_\mu\hat{\pi}\,\hat{\partial}^\mu\hat{\pi}\,\hat{a} + \mathcal{O}\left(\frac{m_\pi^2}{m_K^2}\right)\right], \end{aligned} \tag{42}$$

where we have defined the dimensionless fields

$$\hat{\pi} \equiv \frac{\pi^0}{f_\pi}, \quad \hat{\eta}_{ud} \equiv \left(\frac{1}{\sqrt{3}}\frac{\eta_8}{f_8} + \sqrt{\frac{2}{3}}\frac{\eta_0}{f_0}\right), \quad \hat{a} \equiv \frac{a}{f_a}, \tag{43}$$

the dimensionless LECs,

$$\hat{L}_i \equiv \frac{32m_\eta^2}{f_\pi^2}L_i \sim \mathcal{O}(10^3)L_i, \tag{44}$$

and the dimensionless derivative $\hat{\partial}_\mu \equiv \partial_\mu/m_\eta$. The kinetic terms, omitted in (42), have been canonically normalized. While there is large variation in the literature of the inferred values for L_4 and L_6 from fits to experimental data, depending on assumptions and chosen observables, it is well established from fits to f_K/f_π that L_5 is positive and relatively large, $L_5 \sim (1\text{–}3)\times 10^{-3}$. It is then easy to see from (42) and (44) that the contributions to $\mathcal{A}(\eta \to \pi^0\pi^0 a)$ from the first and second terms in (42) are comparable in magnitude and destructively interfere with each other. This leads to a suppressed rate for $\eta \to \pi^0\pi^0 a$ relative to the naïve $\mathcal{O}(p^2)$ estimation in χPT, which, however, is quite sensitive to the value of L_5. On the other hand, the $\mathcal{O}(p^2)$ contribution to $\mathcal{A}(\eta' \to \pi^0\pi^0 a)$ from the first term in (42) may be subdominant to that of the second term, which is parametrically larger by a factor of $\mathcal{O}(\hat{L}_5 m_{\eta'}^2/m_\eta^2)$. This may lead to an order-of-magnitude enhancement of the rate for $\eta' \to \pi^0\pi^0 a$.

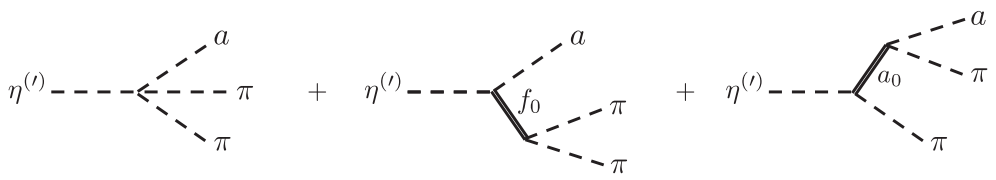

FIG. 2. Contributions to the amplitude $\mathcal{A}(\eta^{(\prime)} \to \pi\pi a)$ in the framework of RχT. Left graph: leading order quartic term. Middle and right graphs: exchange of low-lying scalar resonances.

While it is now straightforward to extract χPT's prediction for $\mathrm{Br}(\eta^{(\prime)} \to \pi^0\pi^0 a)$ using (42), we will instead pivot to RχT, from which ordinary χPT can be recovered by integrating out the low-lying meson resonances. Under the assumption of resonance dominance, RχT predicts that the relevant LECs contributing to $\eta^{(\prime)} \to \pi\pi a$ (L_4, L_5, and L_6) are saturated by the exchange of *scalar* resonances. We will therefore omit the low-lying pseudoscalar, vector, and axial-vector resonances from our discussion. Following the notation in [127], we have

$$\begin{aligned}\mathcal{L}_{\mathrm{R}\chi\mathrm{T}} \supset\ & \frac{f_\pi^2}{4}\mathrm{Tr}[D_\mu U^\dagger D^\mu U] - \frac{1}{2}M_0^2\eta_0^2 \\ & + \frac{f_\pi^2}{4}\mathrm{Tr}[2B_0 M_q(a)U + \mathrm{H.c.}] \\ & + c_d\mathrm{Tr}[SD_\mu U^\dagger D^\mu U] \\ & + c_m\mathrm{Tr}[B_0(SM_q(a) + M_q(a)S)U + \mathrm{H.c.}], \end{aligned} \tag{45}$$

where S is the low-lying $J^{\mathrm{PC}} = 0^{++}$ meson octet,[10]

$$S = \begin{pmatrix} \frac{a_0}{\sqrt{2}} + \frac{f_0}{\sqrt{6}} & a_0^+ & * \\ a_0^- & -\frac{a_0}{\sqrt{2}} + \frac{f_0}{\sqrt{6}} & * \\ * & * & -\frac{f_0}{\sqrt{3/2}} \end{pmatrix}. \tag{46}$$

Above, a_0 and f_0 are shorthand for $a_0(980)$ and $f_0(980)$, respectively [133], and we have not explicitly identified the scalar mesons with nonzero strangeness, since they do not contribute to $\eta^{(\prime)} \to \pi\pi a$.

Accounting for the tadpole-induced nonzero vacuum expectation value of f_0,

$$\langle f_0\rangle = -\frac{4\sqrt{2}}{\sqrt{3}}c_m\frac{(m_K^2 - m_\pi^2/2)}{m_{f_0}^2}, \tag{47}$$

and canonically normalizing the kinetic terms, we can extract from (45) the RχT interactions contributing to $\eta^{(\prime)} \to \pi^0\pi^0 a$,

$$\begin{aligned}\mathcal{L}_{\mathrm{R}\chi\mathrm{T}} \supset\ & \frac{\sqrt{1 + \frac{\widehat{c}_d\widehat{\langle f_0\rangle}}{\sqrt{3/2}}}}{1 + \frac{\widehat{c}_m\widehat{\langle f_0\rangle}}{\sqrt{3/2}}} m_\pi^2 f_\pi^2 (q_{\mathrm{PQ}}^u + q_{\mathrm{PQ}}^d)\frac{m_u m_d}{(m_u + m_d)^2} \\ & \times \left[\widehat{\eta}_{ud}\widehat{\pi}^2\widehat{a} - \frac{2\sqrt{2}}{\sqrt{1 + \frac{\widehat{c}_d\widehat{\langle f_0\rangle}}{\sqrt{3/2}}}}\widehat{c}_m\widehat{a}_0\widehat{\pi}\,\widehat{a} - \frac{2\sqrt{2}}{\sqrt{3}}\widehat{c}_m\widehat{f}_0\,\widehat{\eta}_{ud}\,\widehat{a}\right] \\ & + \frac{m_\eta^2 f_\pi^2}{\sqrt{1 + \frac{\widehat{c}_d\widehat{\langle f_0\rangle}}{\sqrt{3/2}}}}\widehat{c}_d\left[\sqrt{2}\,\widehat{a}_0\,\widehat{\partial}_\mu\widehat{\pi}\,\widehat{\partial}^\mu\widehat{\eta}_{ud} + \frac{1}{\sqrt{6}\sqrt{1 + \frac{\widehat{c}_d\widehat{\langle f_0\rangle}}{\sqrt{3/2}}}}\widehat{f}_0\,\widehat{\partial}_\mu\widehat{\pi}\,\widehat{\partial}^\mu\widehat{\pi}\right], \end{aligned} \tag{48}$$

where, following the notation for the dimensionless fields and derivatives in (42), we have additionally introduced

$$\widehat{a}_0 \equiv \frac{a_0(980)}{f_\pi}, \qquad \widehat{f}_0 \equiv \frac{f_0(980)}{f_\pi} \tag{49}$$

and the dimensionless couplings,

$$\widehat{c}_d \equiv \frac{c_d}{(f_\pi/2)}, \qquad \widehat{c}_m \equiv \frac{c_m}{(f_\pi/2)}. \tag{50}$$

[10]Unlike some studies in the literature, we do not assume the large-N_c limit and do not include a 0^{++} chiral singlet resonance in our analysis. Furthermore, following Refs. [129,130], we consider the broad 0^{++} state $f_0(500)$ [aka $\sigma(500)$] a dynamically generated pole due to strong S-wave interactions, and therefore do not include it as a degree of freedom in (45) and (46).

It is straightforward to recover (42) from (48) by integrating out the scalar resonances and making the following identifications:

$$m_{a_0} \approx m_{f_0} \approx m_S, \tag{51}$$

$$L_4 = -\frac{c_d c_m}{3m_S^2}, \qquad L_5 = \frac{c_d c_m}{m_S^2}, \qquad L_6 = -\frac{c_m^2}{6m_S^2}. \tag{52}$$

Early fits to $a_0(980) \to \pi\eta$ [127], along with large-N_c assumptions and imposition of short-distance constraints [134] (such as sum rules between two-point correlators of two scalar vs two pseudoscalar currents [135], and vanishing of scalar form factors at $q^2 \to \infty$ [136,137]) have been used to estimate the scalar octet couplings to be $|c_d| \sim |c_m| \sim f_\pi/2$, with $c_d c_m > 0$. Here, we conservatively vary these values by $\pm 20\%$ in our calculations of $\Gamma(\eta^{(\prime)} \to \pi\pi a)$, but retain, for simplicity, the assumption of $|c_d| = |c_m|$.

With the relevant interactions in (48), we can then obtain the tree-level amplitude[11] $\mathcal{A}(\eta^{(\prime)} \to \pi\pi a)$ (see Fig. 2),

$$\begin{aligned}
\mathcal{A}_{\eta^{(\prime)}\to\pi\pi a} &\equiv \mathcal{A}(\eta^{(\prime)} \to \pi^0\pi^0 a) = \mathcal{A}(\eta^{(\prime)} \to \pi^+\pi^- a) \\
&= 2C_{\eta^{(\prime)}} \frac{f_\pi}{f_a}(q^u_{\rm PQ} + q^d_{\rm PQ}) \frac{m_\pi^2}{f_\pi^2} \frac{m_u m_d}{(m_u+m_d)^2} \frac{\sqrt{1+\frac{\hat{c}_d\langle \hat{f}_0\rangle}{\sqrt{3/2}}}}{1+\frac{\hat{c}_m\langle \hat{f}_0\rangle}{\sqrt{3/2}}} \\
&\times \left[1 + \frac{2\hat{c}_d\,\hat{c}_m}{1+\frac{\hat{c}_d\langle \hat{f}_0\rangle}{\sqrt{3/2}}}\left(\frac{1}{3}\frac{p_{\pi_1}\cdot p_{\pi_2}}{m_{f_0}^2 - (p_{\pi_1}+p_{\pi_2})^2 - i\Gamma_{f_0} m_{f_0}}\right.\right. \\
&\left.\left. - \frac{p_{\eta^{(\prime)}}\cdot p_{\pi_1}}{m_{a_0}^2 - (p_{\eta^{(\prime)}} - p_{\pi_1})^2 - i\Gamma_{a_0} m_{a_0}} - \frac{p_{\eta^{(\prime)}}\cdot p_{\pi_2}}{m_{a_0}^2 - (p_{\eta^{(\prime)}} - p_{\pi_2})^2 - i\Gamma_{a_0} m_{a_0}}\right)\right],
\end{aligned} \tag{53}$$

where we have neglected subdominant contributions of $\mathcal{O}(m_\pi^2/m_{\eta^{(\prime)}}^2)$. Above, the equality between amplitudes with neutral versus charged pions is due to isospin symmetry; $p_{\eta^{(\prime)}}$, p_{π_1}, and p_{π_2} are relativistic 4-momenta; and

$$C_\eta \equiv \frac{f_\pi}{f_8}\frac{\cos\theta_8}{\sqrt{3}} - \frac{f_\pi}{f_0}\frac{\sin\theta_0}{\sqrt{3/2}}, \tag{54a}$$

$$C_{\eta'} \equiv \frac{f_\pi}{f_8}\frac{\sin\theta_8}{\sqrt{3}} + \frac{f_\pi}{f_0}\frac{\cos\theta_0}{\sqrt{3/2}}. \tag{54b}$$

For the η/η' mixing angles and decay constants above, we will adopt the values from the unconstrained fit in [110], namely, $\theta_8 = -24°$, $\theta_0 = -2.5°$, $f_8 = 1.51 f_\pi$, and $f_0 = 1.29 f_\pi$.

Finally, we can obtain the differential decay rate from (53),

$$\begin{aligned}
d\Gamma(\eta^{(\prime)} \to \pi\pi a) &= \frac{1}{S_{\pi_1\pi_2}}\frac{(2\pi)^4}{2m_{\eta^{(\prime)}}}|\mathcal{A}_{\eta^{(\prime)}\to\pi\pi a}|^2 d\Phi_3(p_{\eta^{(\prime)}}; p_a, p_{\pi_1}, p_{\pi_2}) \\
&= \frac{1}{S_{\pi_1\pi_2}}\frac{1}{(2\pi)^3}\frac{1}{32 m_{\eta^{(\prime)}}^3}|\mathcal{A}_{\eta^{(\prime)}\to\pi\pi a}|^2 dm^2_{\pi_1\pi_2} dm^2_{\pi_2 a},
\end{aligned} \tag{55}$$

where $S_{\pi_1\pi_2}$ is the standard combinatorial factor ($S_{\pi^+\pi^-} = 1$, $S_{\pi^0\pi^0} = 2!$), $d\Phi_3$ is the three-body phase-space differential element, and, when obtaining the total decay rate, the integration over invariant masses $m^2_{\pi_1\pi_2} = (p_{\pi_1} + p_{\pi_2})^2$ and $m^2_{\pi_2 a} = (p_{\pi_2} + p_a)^2 = (p_{\eta^{(\prime)}} - p_{\pi_1})^2$ should be performed over the Dalitz phase space (see, e.g., the PDG review on *Kinematics* [133] for explicit expressions for the Dalitz plot boundaries).

In Fig. 3, we show the branching ratios for $\eta^{(\prime)} \to \pi^0\pi^0 a$, $\eta^{(\prime)} \to \pi^+\pi^- a$ [computed by integrating the differential decay rate in (55) over the final state phase space] as a function of the RχT couplings $\widehat{c}_d, \widehat{c}_m$ of the low-lying scalar octet to the pseudo-Goldstone mesons; see Eqs. (45), (48), and (50). As mentioned previously, we assume, for simplicity, that $\widehat{c}_d = \widehat{c}_m$, and vary their magnitudes by $\pm 20\%$ around their expected values of $|\widehat{c}_d| = |\widehat{c}_m| = 1$ in the large-N_c limit. The range covered by the bands are due to the uncertainties in the masses and widths of the scalar resonances $a_0(980)$ and $f_0(980)$—following the PDG [133], we varied these parameters independently within the following ranges: $m_{a_0}, m_{f_0} = (960\text{–}1000)$ MeV, $\Gamma_{a_0} = (40\text{–}100)$ MeV, $\Gamma_{f_0} = (10\text{–}200)$ MeV.

The lack of predictive power of our treatment, with an estimated range of branching ratios spanning 2 orders of

[11] We ignore corrections to $\mathcal{A}(\eta^{(\prime)} \to \pi\pi a)$ from $\pi\pi$ final state rescattering, based on the conclusions from [116,118] that these effects correct the $\eta \to 3\pi$ amplitude by modest amounts of $\mathcal{O}(10\%)$, and on Ref. [117], which finds somewhat larger rescattering corrections, of $\sim$70%, which are still subdominant relative to other sources of uncertainties in our estimations.

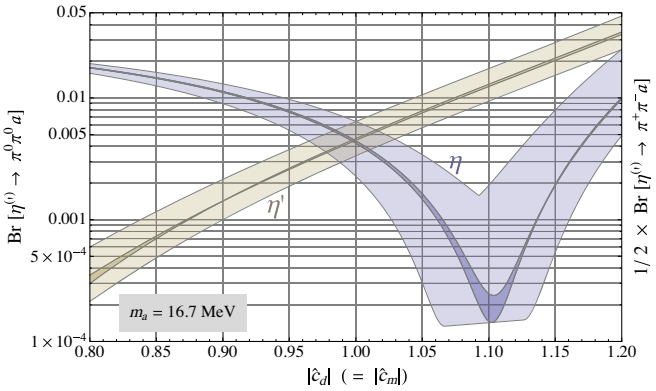

FIG. 3. Estimated branching ratios for $\eta^{(\prime)} \to \pi\pi a$ as a function of the scalar octet couplings to the light pseudoscalar mesons, cf. (45), (48), and (50). The bands result from varying the masses and widths of the scalar resonances, a_0 and f_0, within their experimental uncertainties. For the dark narrow bands, their masses are fixed to $m_{a_0} = m_{f_0} = 980$ MeV, and their widths are varied within the ranges $\Gamma_{a_0} = (40\text{–}100)$ MeV, $\Gamma_{f_0} = (10\text{–}200)$ MeV. The broader bands result from additionally varying their masses within the ranges $m_{a_0}, m_{f_0} = (960\text{–}1000)$ MeV.

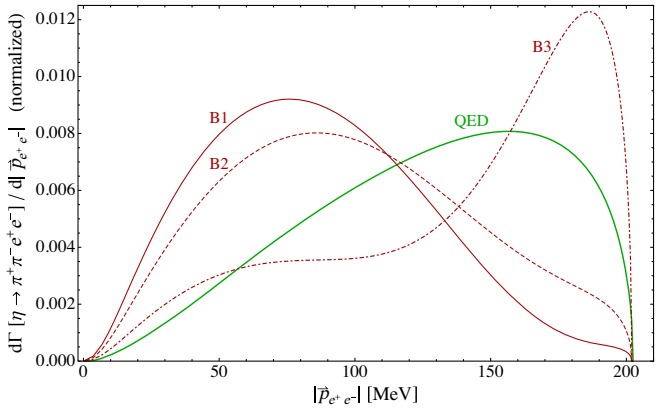

FIG. 4. The differential rate for $\eta \to \pi^+\pi^- a$ as a function of $|\vec{p}_{e^+e^-}| \equiv |\vec{p}_{e^+} + \vec{p}_{e^-}| = \vec{p}_a$, for three benchmark choices of RχT parameters specified in Table I. For comparison, we also show the differential rate of the SM process $\eta \to \pi^+\pi^- e^+ e^-$, labeled "QED."

magnitude, $\mathrm{Br}(\eta^{(\prime)} \to \pi\pi a) \sim \mathcal{O}(10^{-4}\text{–}10^{-2})$, is due to the χPT and RχT parameters falling on a special range of values that, within uncertainties, can lead to substantial destructive inference between the LO amplitude and the amplitudes originating from exchange of low-lying scalar resonances. This is perhaps unsurprising, considering that even the SM hadronic decays of the η and η' could not be correctly predicted, but only "postdicted," and their experimentally determined branching ratios and Dalitz plot parameters have been used to verify the validity of various treatments and assumptions, such as RχT, QCD sum rules, large-N_c limit, dispersive methods, etc. [116–126].

In particular, the upper range of our estimations, $\mathrm{Br}(\eta^{(\prime)} \to \pi\pi a) \sim \mathcal{O}(10^{-2})$, is probably excluded or in tension with observations, though no dedicated searches for an e^+e^- resonance in $\eta^{(\prime)} \to \pi\pi e^+e^-$ final states have ever been performed, to the best of our knowledge. However, the lower range $\mathrm{Br}(\eta^{(\prime)} \to \pi\pi a) \sim \mathcal{O}(10^{-4}\text{–}10^{-3})$ likely remains experimentally allowed, and within the sensitivity of upcoming η/η' factories, such as the JLab Eta Factory (JEF) and the REDTOP experiment.

The most recent and precise measurement of the SM decay $\eta \to \pi^+\pi^-(\gamma^* \to e^+e^-)$, which shares the same final state of $\eta \to \pi^+\pi^- a$, was performed by the KLOE Collaboration at the Frascati ϕ-factory DAΦNE [138]. While their measurement yielded $\mathrm{Br}(\eta \to \pi^+\pi^- e^+e^-) = (2.68 \pm 0.09_{\mathrm{stat}} \pm 0.07_{\mathrm{syst}}) \times 10^{-4}$, it is nontrivial to infer any bounds from this analysis on $\mathrm{Br}(\eta \to \pi^+\pi^- a)$. This is because, without proper Monte Carlo simulations, one cannot determine how the background rejection requirements would have affected the $\eta \to \pi^+\pi^- a$ signal efficiency. In particular, this search rejected events with $m_{e^+e^-} < 15$ MeV whose reconstructed e^+e^- vertex was within a 2.5 cm distance from the beampipe. This cut could have significantly impacted the acceptance of the axion signal, depending on the $m_{e^+e^-}$ experimental resolution. Other event selection requirements on the momenta of the $\pi^\pm$ and $e^\pm$ charged tracks could in principle have rejected a large fraction of the axion signal as well.

An earlier measurement of $\mathrm{Br}(\eta \to \pi^+\pi^-(\gamma^* \to e^+e^-))$ by the CELSIUS/WASA Collaboration observed, in hindsight, an upward fluctuation of the expected signal [139,140]. Indeed, considering KLOE's more precise measurement of this branching ratio, the CELSIUS/WASA analysis should have expected 10 SM signal events. It observed 24 events in the signal region, of which it determined that 7.7 were from background, and 16.3 were from the SM signal. Assuming, conservatively, that the 14 "excess events" were instead due to $\eta \to \pi^+\pi^- a$ decays, and taking into account the relative signal acceptance due to the minimum transverse momentum requirement of $|\vec{p}_T| > 20$ MeV for charged particles,[12] we estimate that branching ratios as large as $\mathrm{Br}(\eta \to \pi^+\pi^- a) \sim (1-3) \times 10^{-3}$ could be compatible with the CELSIUS/WASA measurement, although, without access to nonpublic information on details of the experimental analysis, this estimation is at the level of an educated guess.

Finally, the two existing measurements of $\mathrm{Br}(\eta' \to \pi^+\pi^-(\gamma^* \to e^+e^-))$, performed independently by the

[12]We performed a simple MC event simulation to estimate the geometric acceptance resulting from the event selection requirement of $|\vec{p}_T^{\,e^\pm}| > 20$ MeV, properly taking the momentum dependence of the amplitudes into account. This was done for both the SM signal using the amplitude in [139], as well as for the axion signal, assuming a few RχT benchmark parameters (see discussion below). We neglected contributions to the signal efficiency from other event selection requirements and worked in the approximation of η mesons decaying at rest.

TABLE I. Benchmarked RχT parameters for the examples in Fig. 4 and the resulting prediction for the total decay rate of $\eta \to \pi^+\pi^- a$.

	m_{a_0} (MeV)	Γ_{a_0} (MeV)	m_{f_0} (MeV)	Γ_{f_0} (MeV)	$\lvert\widehat{c}_d\rvert = \lvert\widehat{c}_m\rvert$	$\mathrm{Br}(\eta \to \pi^+\pi^- a)$
B1	980	40	980	200	1.125	0.96×10^{-3}
B2	980	50	980	100	1.125	1.1×10^{-3}
B3	1000	50	1000	100	1.125	0.49×10^{-3}

CLEO [141] and BESIII [142] Collaborations, were combined by the PDG [133] to give $\mathrm{Br}(\eta' \to \pi^+\pi^- e^+ e^-) = (2.4^{+1.3}_{-0.9}) \times 10^{-3}$. However, both experimental analyses reported large external photon-conversion backgrounds in the signal region, peaked in the range $m_{e^+e^-} =$ (8–25) MeV (CLEO; see Fig. 2(d) of [141]) and $m_{e^+e^-} =$ (10–20) MeV (BESIII; see Fig. 2 of [142]). Events falling within these $m_{e^+e^-}$ windows were excluded from the analyses' inference of the SM branching ratio. Since events from $\eta' \to \pi^+\pi^- a$ would have fallen precisely in this region where the photon conversion background peaked, it is difficult to estimate how strong a potential axion signal could have been. Simply requiring that the axion signal strength does not overpredict the number of events attributed to photon-conversion yields a conservative limit of $\mathrm{Br}(\eta' \to \pi^+\pi^- a) \lesssim$ few $\times 10^{-2}$, which is not particularly useful.

We end this section by remarking that an additional challenge with estimating the sensitivity of current and future experiments to $\eta^{(\prime)} \to \pi\pi a$ is the uncertainty in the final state Dalitz phase space, which affects the signal acceptance resulting from event selection cuts. Consider, for instance, the differential decay rate $d\Gamma(\eta \to \pi^+\pi^- a)/d|\vec{p}_a|$ as a function of the axion's 3-momentum $|\vec{p}_a|$. The dependence of this rate on $|\vec{p}_a| = |\vec{p}_{e^+} + \vec{p}_{e^-}| \equiv |\vec{p}_{e^+e^-}|$ varies dramatically depending of the numerical values chosen for the masses, widths, and couplings of the scalar resonances a_0 and f_0. We illustrate this effect in Fig. 4, where we plot the differential decay rate $d\Gamma(\eta \to \pi^+\pi^- e^+ e^-)/d|\vec{p}_{e^+e^-}|$ as a function of $|\vec{p}_{e^+e^-}|$ for three different RχT benchmarks—corresponding to different choices of masses and widths for a_0 and f_0 within uncertainties (see Table I)—as well as for the SM decay $\eta \to \pi^+\pi^-(\gamma^* \to e^+e^-)$ [107] (labeled as "QED" in Fig. 4). While these different benchmark points yield close predictions for $\mathrm{Br}(\eta \to \pi^+\pi^- a)$, their predictions for $d\Gamma(\eta \to \pi^+\pi^- a)/d|\vec{p}_a|$ differ dramatically, as shown in Fig. 4. In particular, for high enough cuts on the charged lepton momenta $\vec{p}_{e^\pm}$, the signal acceptance of benchmark B1 could be significantly lower than that of B3 (and of the SM decay $\eta \to \pi^+\pi^-\gamma^*$). Indeed, this could lead to a variation of as much as an order of magnitude in the expected sensitivity of experimental searches.

V. KAON DECAYS

We conclude our study by exploring signals of the piophobic QCD axion in rare kaon decays. Although the main focus of ongoing and near-future rare kaon decay experiments—such as NA62 at CERN [143] and KOTO at J-PARC [144]—has been on $K \to \pi\nu\bar{\nu}$, there is an under explored opportunity to search for BSM resonances in e^+e^- final states with low $m_{e^+e^-}$, motivated not only by the piophobic QCD axion, but also by visibly decaying ALPs and dark photons more generally [42]. Furthermore, the highly suppressed $a \to \gamma\gamma$ decay mode might be a competitive final state in kaon decay searches for which $\gamma\gamma$ backgrounds in the $m_{\gamma\gamma} \sim 17$ MeV signal region are tamer than the e^+e^- backgrounds. In such cases, final states with $K \to (a \to \gamma\gamma) + \mathrm{SM}$ can be obtained by combining the relevant branching ratios $\mathrm{Br}(K \to a + \mathrm{SM})$ estimated in this section with $\mathrm{Br}(a \to \gamma\gamma)$ in (13).

The appearance of the axion in kaon decay final states occurs via mixing with the neutral octet mesons, π^0, η, and η'. Therefore, the axionic amplitudes can be obtained from ordinary SM amplitudes properly reweighted by axion-meson mixing angles. While this prescription is straightforward for estimating "axio-leptonic" kaon decays such as $K^+ \to \mu^+\nu_\mu a$ (as we will show in Sec. V A), it is ambiguous for "axio-hadronic" kaon decays such as $K^+ \to \pi^+ a$, $K^0_{S,L} \to \pi^0 a$, and $K^0_L \to \pi\pi a$. Firstly, the two-body hadronic width of the CP-even neutral kaon, $\Gamma(K^0_S \to \pi^0\pi^0, \pi^+\pi^-) \approx 0.73 \times 10^{-5}$ eV, is enhanced by roughly 3 orders of magnitude relative to the two-body hadronic width of the charged kaon, $\Gamma(K^+ \to \pi^+\pi^0) \approx 1.1 \times 10^{-8}$ eV. In χPT, this enhancement is parametrized as a large disparity in the magnitudes of the Wilson coefficients of the possible $\Delta S = 1$ operators [112,145–147]. Specifically, the coefficient of an $SU(3)_\chi$-octet ($\Delta I = 1/2$) operator is larger than the coefficient of the leading order 27-plet ($\Delta I = 3/2$) operator by a factor of $\sim$30. Secondly, phenomenologically, there are at least two choices of $\Delta S = 1$ octet operators that could be responsible for this so-called "octet enhancement" (aka "$\Delta I = 1/2$ enhancement") in kaon decays [148–150], namely,

$$O_8^{(\Delta S=1)} = g_8 f_\pi^2 \mathrm{Tr}(\lambda_{ds}\partial_\mu U \partial^\mu U^\dagger) + \mathrm{H.c.}, \tag{56a}$$

$$O_8^{\prime(\Delta S=1)} = -g_8' \frac{f_\pi^2}{\Lambda^2} \mathrm{Tr}(\lambda_{ds} 2B_0 M_q^\dagger(a) U^\dagger)\mathrm{Tr}(\partial_\mu U \partial^\mu U^\dagger) + \mathrm{H.c.}, \tag{56b}$$

where $\lambda_{ds} \equiv (\lambda_6 + i\lambda_7)/2$, $\Lambda \sim 2m_K$ is a natural χPT cutoff, and the operators above occur at different orders in the chiral expansion: O_8 at $\mathcal{O}(p^2)$ and O_8' at $\mathcal{O}(p^4)$. Fitting existing data on $K \to \pi\pi$ and $K \to \pi\pi\pi$, while treating the coefficients g_8 and g_8' in (56) on equal footing, yields

$|g_8 + g_8'| \simeq 0.78 \times 10^{-7}$ [151,152]. In order to break this degeneracy in the fit, one must invoke the standard assumption under naïve power counting that $\Delta S = 1$ octet enhancement should appear at lowest order in the chiral expansion, and therefore, $g_8' \ll g_8 \Rightarrow |g_8| \simeq 0.78 \times 10^{-7}$. However, there is no first principles derivation of this choice, and it could be incorrect. For example, in the Resonance Chiral Theory framework discussed in the previous section, it is easy to speculate that the origin of $\Delta S = 1$ octet enhancement could be due to the weak interactions inducing a mixing between K_S^0 and a broad $J^{PC} = 0^{++}$ resonance, such as the $\sigma(500)$.[13] Upon integration of the low-lying resonances, this effect would be captured by the operator O_8' in (56b), leading instead to $g_8 \ll g_8' \Rightarrow |g_8'| \simeq 0.78 \times 10^{-7}$.

This ambiguity directly affects predictions for rare kaon decays to the piophobic axion, since the $\Delta S = 1$ octet operators O_8 and O_8' contribute differently to the amplitudes $\mathcal{A}(K^+ \to \pi^+ a)$, $\mathcal{A}(K_{S,L}^0 \to \pi^0 a)$, and $\mathcal{A}(K_L^0 \to \pi\pi a)$. In what follows, we will estimate the rates for various axionic kaon decays in both scenarios, $g_8 \gg g_8'$ and $g_8 \ll g_8'$. We will show that in the case of $g_8 \gg g_8'$, all amplitudes $\mathcal{A}(K^+ \to \pi^+ a)$, $\mathcal{A}(K_{S,L}^0 \to \pi^0 a)$, and $\mathcal{A}(K_L^0 \to \pi\pi a)$ are octet enhanced, leading to higher axionic kaon decay rates, and when relevant, more stringent constraints on the mixing angles $\theta_{a\eta_{ud}}$ and $\theta_{a\eta_s}$. Conversely, in the scenario with $g_8 \ll g_8'$, the rates $\Gamma(K^+ \to \pi^+ a)$ and $\Gamma(K_{S,L}^0 \to \pi^0 a)$ are significantly reduced, relaxing the otherwise strong constraints on $\theta_{a\eta_{ud}}$ and offering an exciting prospect for searching for these signals in near-future rare kaon decay experiments.

In upcoming subsections, we will normalize the calculated axio-hadronic rates to analogous kaon decay rates in the SM. For later reference, we quote here the dependence of the relevant SM kaon decay amplitudes on g_8, g_8', as well as g_{27}, the coefficient of the $\Delta S = 1$ 27-plet operator at $\mathcal{O}(p^2)$ in χPT, which is given by

$$O_{27}^{(\Delta S=1)} = g_{27} f_\pi^2 T_{kl}^{ij} (U^\dagger \partial_\mu U)_i^k (U^\dagger \partial^\mu U)_j^l. \tag{57}$$

Above, T_{kl}^{ij} are Clebsch-Gordan coefficients that project the 27-plet, $\Delta I = 3/2$ part of the interaction [146]. The contributions from (56a), (56b), and (57) to the two-body hadronic kaon decays of interest are [151,153]

$$\mathcal{A}(K_S^0 \to \pi^+\pi^-) = 2(g_8 + g_8' + g_{27})\frac{m_K^2}{f_\pi} - 2(g_8 + 2g_8' + g_{27})\frac{m_\pi^2}{f_\pi}, \tag{58}$$

$$\mathcal{A}(K^+ \to \pi^+\pi^0) = 3 g_{27} \frac{(m_K^2 - m_\pi^2)}{f_\pi}. \tag{59}$$

As alluded to earlier, the hadronic K^+ decay amplitude is not octet enhanced, and its consequent narrow width relative to that of K_S^0 is parametrized by a hierarchy between the 27-plet and octet coefficients,

$$g_{27} \simeq 2.5 \times 10^{-9} \approx 0.032 \times |g_8 + g_8'|. \tag{60}$$

Finally, for the relevant hadronic three-body decay of K_L^0, we have [151,153]

$$\mathcal{A}(K_L^0 \to \pi^+\pi^-\pi^0) = \frac{(g_8 + g_8' + 2g_{27})}{3}\frac{m_K^2}{f_\pi^2} - g_8'\frac{m_\pi^2}{f_\pi^2} + \left(g_8 + g_8' - \frac{5}{2}g_{27}\right)\frac{m_\pi^2 Y}{f_\pi^2}, \tag{61}$$

where Y is one of the standard Dalitz plot variables, defined as

$$Y \equiv (s_3 - s_0)/m_\pi^2, \tag{62a}$$

$$s_i \equiv (p_K - p_i)^2|_{i=1,2,3}, \tag{62b}$$

$$s_0 \equiv \frac{(s_1 + s_2 + s_3)}{3}, \tag{62c}$$

with p_1 and p_2 referring to the four-momenta of the charged pions, and p_3 the four-momentum of the neutral daughter particle,[14] in this case π^0.

A. K^+ decays

1. Axio-leptonic K^+ decays

The amplitude for the axio-leptonic decay $K^+ \to \ell^+ \nu_\ell a$ can be easily related to the SM semileptonic amplitudes via the Ademollo-Gatto theorem [154], which states that the matrix elements of flavor-changing electroweak current operators can only deviate from their $SU(3)_\chi$-symmetric values to second order in chiral symmetry breaking [155,156].

This implies that, at zero momentum transfer, the following $SU(3)_\chi$ relations hold:

$$\langle \eta_8 | \bar{s}\gamma^\mu u | K^+ \rangle|_{q^2=0} = \sqrt{3}\langle \pi^0 | \bar{s}\gamma^\mu u | K^+ \rangle|_{q^2=0} + \mathcal{O}(\epsilon^2), \tag{63a}$$

$$\langle \eta_0 | \bar{s}\gamma^\mu u | K^+ \rangle|_{q^2=0} = \mathcal{O}(\epsilon^2), \tag{63b}$$

where ϵ is a measure of $SU(3)_\chi$ breaking. Then, since $|a\rangle = \theta_{a\pi}|\pi^0\rangle + \theta_{a\eta_8}|\eta_8\rangle + \theta_{a\eta_0}|\eta_0\rangle$, we have

[13] Indeed, a naïve dimensional analysis estimation of $g_8' \sim |G_F \sin\theta_c f_\pi^2 \Lambda^2 / m_{0^{++}}^2| \sim \mathcal{O}(10^{-7})$ does not immediately rule out this hypothesis. It is unclear whether a Dalitz plot analysis of $K_L^0 \to 3\pi$ data could distinguish it from the alternative description of octet enhancement.

[14] Note that in Sec. V C 2, p_3 will refer to the axion's four-momentum.

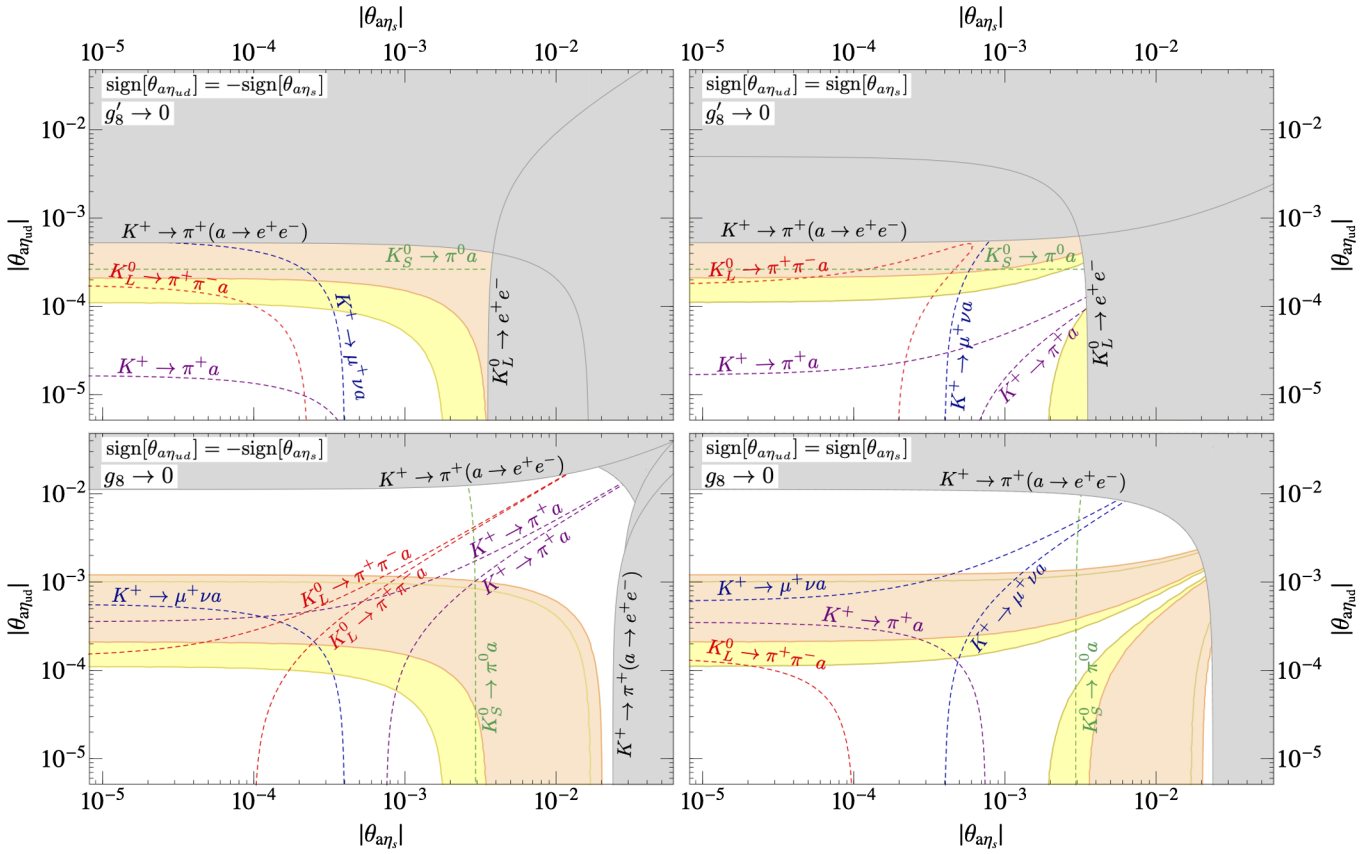

FIG. 5. (Disclaimer: not intended as a realistic experimental sensitivity projection.) The dashed lines show the reach of various axionic kaon decays modes in the parameter space of the axion isoscalar couplings, assuming a common branching ratio sensitivity benchmark of 10^{-8} for all decay channels. The upper (lower) plots assume that octet enhancement in χPT is realized through operator O_8 (O_8') defined in (56a) ((56b)). The left (right) plots assume opposite (same) relative sign between $\theta_{a\eta_{ud}}$ and $\theta_{a\eta_s}$. The orange and yellow bands favored by the ^{8}Be and ^{4}He anomalies are the same as in Fig. 1. The shaded gray regions are excluded by the conservative upper bound $\text{Br}(K^+ \to \pi^+(a \to e^+e^-)) \lesssim 10^{-5}$ and by the observed rate for $K_L^0 \to e^+e^-$, cf. (91).

$$\begin{aligned}\langle a|\bar{s}\gamma^\mu u|K^+\rangle|_{q^2=0} &= (\theta_{a\pi} + \sqrt{3}\theta_{a\eta_8})\langle\pi^0|\bar{s}\gamma^\mu u|K^+\rangle|_{q^2=0} + \mathcal{O}(\epsilon^2),\\ &= (\theta_{a\pi} + \theta_{a\eta_{ud}} - \sqrt{2}\theta_{a\eta_s})\langle\pi^0|\bar{s}\gamma^\mu u|K^+\rangle|_{q^2=0} + \mathcal{O}(\epsilon^2).\end{aligned} \tag{64}$$

Neglecting the difference in phase space, as well as finite momentum-transfer and $SU(3)_\chi$ breaking corrections, which amount to $\mathcal{O}(10\%)$ [153], it then follows from (64) that

$$\begin{aligned}&\text{Br}(K^+ \to \ell^+\nu_\ell a)\\ &\quad\approx |\theta_{a\pi} + \theta_{a\eta_{ud}} - \sqrt{2}\theta_{a\eta_s}|^2 \text{Br}(K^+ \to \ell^+\nu_\ell\pi^0),\end{aligned} \tag{65}$$

In the specific case of a muonic final state, (65) yields

$$\text{Br}(K^+ \to \mu^+\nu_\mu a) \approx 0.84 \times 10^{-8}\left|\frac{\theta_{a\pi} + \theta_{a\eta_{ud}} - \sqrt{2}\theta_{a\eta_s}}{5\times 10^{-4}}\right|^2. \tag{66}$$

In Fig. 5, we show the hypothetical reach of $K^+ \to \mu^+\nu_\mu a$ to the axion isoscalar mixing angles, assuming an experimental sensitivity to branching ratios $\text{Br}(K^+ \to \mu^+\nu_\mu a) \gtrsim 10^{-8}$. Note that this branching ratio sensitivity figure has been chosen to facilitate comparison between different axionic kaon decay modes (to be discussed in upcoming subsections) and is not informed by any experimental sensitivity projections.

2. *Axio-hadronic K^+ decays*

For axio-hadronic kaon decays, we must first obtain the contributions from operators (56a), (56b), and (57) to the amplitudes for $K^+ \to \pi^+\varphi^*$ ($\varphi = \pi^0, \eta_{ud}, \eta_s$). Putting K^+ and π^+ on shell, we have

$$\begin{aligned}&\mathcal{A}(K^+ \to \pi^+\pi^{0*})\\ &\quad= 3g_{27}\frac{m_K^2}{f_\pi} - (g_8 + 4g_{27})\frac{m_\pi^2}{f_\pi} + (g_8 + g_{27})\frac{p_{\pi^0}^2}{f_\pi},\end{aligned} \tag{67a}$$

$$\mathcal{A}(K^+ \to \pi^+ \eta_{ud}^*) = (2g_8 + 3g_{27})\frac{m_K^2}{f_\pi} - (g_8 + 2g_{27})\frac{m_\pi^2}{f_\pi} - (g_8 + g_{27})\frac{p_{\eta_{ud}}^2}{f_\pi}, \tag{67b}$$

$$\mathcal{A}(K^+ \to \pi^+ \eta_s^*) = \sqrt{2}g_{27}\frac{m_K^2}{f_\pi} - \sqrt{2}(g_8 + 2g_{27})\frac{m_\pi^2}{f_\pi} + \sqrt{2}(g_8 + g_{27})\frac{p_{\eta_s}^2}{f_\pi}. \tag{67c}$$

The axionic decay $K^+ \to \pi^+ a$ is then induced by these amplitudes via axion-meson mixing,

$$\begin{aligned}\mathcal{A}(K^+ \to \pi^+ a) = {} & \theta_{a\pi}\mathcal{A}(K^+ \to \pi^+ \pi^{0*})|_{p_{\pi^0}^2 = m_a^2} \\ & + \theta_{a\eta_{ud}}\mathcal{A}(K^+ \to \pi^+ \eta_{ud}^*)|_{p_{\eta_{ud}}^2 = m_a^2} \\ & + \theta_{a\eta_s}\mathcal{A}(K^+ \to \pi^+ \eta_s^*)|_{p_{\eta_s}^2 = m_a^2}.\end{aligned} \tag{68}$$

Note that (68) depends on g_8 but not on g_8'. This implies that $\mathcal{A}(K^+ \to \pi^+ a)$ is only octet enhanced in the scenario with $g_8 \gg g_8'$, i.e., in the standard realization of octet enhancement in χPT via O_8. In this case, using (58) and taking $g_8' \to 0$ for simplicity, we can approximate (68) as

$$|\mathcal{A}(K^+ \to \pi^+ a)|^2|_{\text{octet enh}} \approx \frac{1}{K_{\pi\pi}}|\mathcal{A}(K_S^0 \to \pi^+\pi^-)|^2 \frac{|2g_8\theta_{a\eta_{ud}} + \sqrt{2}\theta_{a\eta_s}(g_{27} - g_8\frac{m_\pi^2}{m_K^2})|^2}{|2(g_8 + g_{27})|^2}, \tag{69}$$

where $K_{\pi\pi} \sim 3$ corrects for the fact that strong s-wave $\pi\pi$ final state interaction, present in $K_S^0 \to \pi^+\pi^-$, is absent in $K^+ \to \pi^+ a$ [62]. With (69) and (60), we finally obtain

$$\begin{aligned}\text{Br}(K^+ \to \pi^+ a)|_{\text{octet enh}} &\approx \left.\frac{|\mathcal{A}(K^+ \to \pi^+ a)|^2}{|\mathcal{A}(K_S^0 \to \pi^+\pi^-)|^2}\right|_{(69)} \text{Br}(K_S^0 \to \pi^+\pi^-)\frac{\Gamma_{K_S^0}}{\Gamma_{K^+}}\frac{\vec{p}_a}{\vec{p}_\pi} \\ &\approx 0.9 \times 10^{-5}\left|\frac{\theta_{a\eta_{ud}} - 0.032\theta_{a\eta_s}}{5 \times 10^{-4}}\right|^2.\end{aligned} \tag{70}$$

In the scenario with $g_8 \ll g_8'$, $\mathcal{A}(K^+ \to \pi^+ a)$ is not octet enhanced. Since g_8 is then expected to be of the same magnitude as g_{27}, there might be non-negligible interference between the contributions stemming from O_8 and O_{27}. For simplicity, we will ignore this effect and consider the limiting case of $g_8 \to 0$, when O_{27} provides the dominant contribution to axio-hadronic K^+ decays. In this case, using (59), (68) can be approximated as

$$|\mathcal{A}(K^+ \to \pi^+ a)|^2|_{27\text{-plet}} \approx \frac{1}{K_{\pi\pi}}|\mathcal{A}(K^+ \to \pi^+\pi^0)|^2\left|\theta_{a\pi} + \theta_{a\eta_{ud}} + \frac{\sqrt{2}}{3}\theta_{a\eta_s}\right|^2, \tag{71}$$

from which it follows that

$$\begin{aligned}\text{Br}(K^+ \to \pi^+ a)|_{27\text{-plet}} &\approx \left.\frac{|\mathcal{A}(K^+ \to \pi^+ a)|^2}{|\mathcal{A}(K^+ \to \pi^+\pi^0)|^2}\right|_{(71)} \text{Br}(K^+ \to \pi^+\pi^0)\frac{\vec{p}_a}{\vec{p}_\pi} \\ &\approx 2 \times 10^{-8}\left|\frac{\theta_{a\pi} + \theta_{a\eta_{ud}} + \frac{\sqrt{2}}{3}\theta_{a\eta_s}}{5 \times 10^{-4}}\right|^2.\end{aligned} \tag{72}$$

In Figs. 1 and 5, we show the excluded parameter space for the axion's isoscalar mixing angles—assuming a conservative experimental bound of $\text{Br}(K^+ \to \pi^+ a) \lesssim 10^{-5}$ (see discussion in [46])—for the two assumed scenarios of octet enhancement in χPT which resulted in (70) and (72).

We also show in Fig. 5 the hypothetical reach of $K^+ \to \pi^+ a$ to the axion isoscalar mixing angles, assuming an experimental sensitivity[15] to branching ratios $\text{Br}(K^+ \to \pi^+ a) \gtrsim 10^{-8}$. The $K^+ \to \pi^+ a$ contours in Fig. 5 make evident that this axionic kaon decay channel is one of the most sensitive in probing the piophobic QCD axion, and that updating the three-decades-old bounds on $K^+ \to \pi^+ e^+ e^-$ with $m_{e^+e^-} \lesssim 50$ MeV [157–159] could cover presently unexplored and well-motivated parameter space of light BSM sectors.

B. K_S^0 decays

The axio-hadronic decays of the CP-even neutral kaon can be estimated via an analogous prescription as the one used in Sec. V A 2. First, we obtain the contributions to $\mathcal{A}(K_S^0 \to \pi^0\varphi^*)$, $\varphi = \pi^0, \eta_{ud}, \eta_s$, from operators (56a), (56b), and (57). With K_S^0 and π^0 on shell, we have

$$\begin{aligned}\mathcal{A}(K_S^0 \to \pi^0\pi^{0*}) = {} & (g_8 + g_8' - 2g_{27})\left(\frac{2m_K^2}{f_\pi} - \frac{m_\pi^2}{f_\pi} - \frac{p_{\pi^{0*}}^2}{f_\pi}\right) \\ & - g_8'\left(\frac{m_\pi^2}{f_\pi} + \frac{p_{\pi^{0*}}^2}{f_\pi}\right),\end{aligned} \tag{73a}$$

$$\begin{aligned}\mathcal{A}(K_S^0 \to \pi^0\eta_{ud}^*) = {} & -2g_8\frac{m_K^2}{f_\pi} + (g_8 + 2g_{27})\frac{m_\pi^2}{f_\pi} \\ & + (g_8 - 2g_{27})\frac{p_{\eta_{ud}}^2}{f_\pi},\end{aligned} \tag{73b}$$

$$\begin{aligned}\mathcal{A}(K_S^0 \to \pi^0\eta_s^*) = {} & -4\sqrt{2}g_{27}\frac{m_K^2}{f_\pi} + \sqrt{2}(g_8 + 2g_{27})\frac{m_\pi^2}{f_\pi} \\ & - \sqrt{2}(g_8 - 2g_{27})\frac{p_{\eta_s}^2}{f_\pi}.\end{aligned} \tag{73c}$$

The axionic decay $K_S^0 \to \pi^0 a$ is then induced by these amplitudes via axion-meson mixing,

[15]This choice of branching ratio sensitivity benchmark of 10^{-8} is intended to facilitate comparison between different axionic kaon decay modes and is not informed by any experimental sensitivity projections.

$$\mathcal{A}(K_S^0 \to \pi^0 a) = \theta_{a\pi}\mathcal{A}(K_S^0 \to \pi^0\pi^{0*})|_{p^2_{\pi^{0*}}=m_a^2} + \theta_{a\eta_{ud}}\mathcal{A}(K_S^0 \to \pi^0\eta^*_{ud})|_{p^2_{\eta_{ud}}=m_a^2} + \theta_{a\eta_s}\mathcal{A}(K_S^0 \to \pi^0\eta^*_s)|_{p^2_{\eta_s}=m_a^2}. \quad (74)$$

Note that the only occurrence of g_8' in (74) stems from the axion-pion mixing contribution in (73a), and, as such, it is suppressed by the small $\theta_{a\pi}$ mixing angle. Because of this, $\mathcal{A}(K_S^0 \to \pi^0 a)$ parallels the behavior of $\mathcal{A}(K^+ \to \pi^+ a)$ of only being octet enhanced in the scenario with $g_8 \gg g_8'$. In this case, using (59), we can approximate (74) as

$$|\mathcal{A}(K_S^0 \to \pi^0 a)|^2|_{\text{octet enh}} \approx \frac{1}{K_{\pi\pi}}|\mathcal{A}(K_S^0 \to \pi^+\pi^-)|^2|\theta_{a\eta_{ud}}|^2 \quad (75)$$

to then obtain

$$\begin{aligned}\text{Br}(K_S^0 \to \pi^0 a)|_{\text{octet enh}} &\approx \left.\frac{|\mathcal{A}(K_S^0 \to \pi^0 a)|^2}{|\mathcal{A}(K_S^0 \to \pi^+\pi^-)|^2}\right|_{(75)} \text{Br}(K_S^0 \to \pi^+\pi^-)\frac{\vec{p}_a}{\vec{p}_\pi} \\ &\approx 6\times 10^{-8}\left|\frac{\theta_{a\eta_{ud}}}{5\times 10^{-4}}\right|^2. \end{aligned} \quad (76)$$

In the alternative scenario with $g_8' \gg g_8$, when g_8 and g_{27} are expected to have comparable magnitudes, there will be non-negligible interference between the O_8 and O_{27} contributions to the amplitudes (73b) and (73c). For simplicity, we again consider the limiting case of $g_8 \to 0$ to arrive at the following approximation:

$$|\mathcal{A}(K_S^0 \to \pi^0 a)|^2|_{27\text{-plet}} \approx \frac{1}{K_{\pi\pi}}|\mathcal{A}(K_S^0 \to \pi^+\pi^-)|^2 \times \frac{|2g_8'\theta_{a\pi} - 4\sqrt{2}g_{27}\theta_{a\eta_s}|^2}{|2(g_8'+g_{27})|^2}, \quad (77)$$

from which it follows that

$$\begin{aligned}\text{Br}(K_S^0 \to \pi^0 a)|_{27\text{-plet}} &\approx \left.\frac{|\mathcal{A}(K_S^0 \to \pi^0 a)|^2}{|\mathcal{A}(K_S^0 \to \pi^+\pi^-)|^2}\right|_{(77)} \text{Br}(K_S^0 \to \pi^+\pi^-)\frac{\vec{p}_a}{\vec{p}_\pi} \\ &\approx 0.8\times 10^{-8}\left|\frac{\theta_{a\eta_s} - 11\theta_{a\pi}}{2\times 10^{-3}}\right|^2. \end{aligned} \quad (78)$$

Note that in (78) the contribution from axion-pion mixing is non-negligible despite the suppression of $\theta_{a\pi}$ relative to $\theta_{a\eta_s}$. As alluded to earlier, this is because (73a) is the only octet-enhanced amplitude contributing to $K_S^0 \to \pi^0 a$ in the scenario with $g_8' \gg g_8$.

Present bounds on $K_S^0 \to \pi^0(a \to e^+e^-)$ are difficult to infer from published experimental analyses of this final state. The observation of the SM process $K_S^0 \to \pi^0 e^+e^-$ by the NA48/1 experiment at the CERN SPS [160], with a measured branching ratio of $\text{Br}(K_S^0 \to \pi^0 e^+e^-) = (5.8^{+2.9}_{-2.4})\times 10^{-9}$, rejected events with $m_{e^+e^-} < 165$ MeV. In prior searches for this decay mode, the published analyses by NA31 [161] and NA48 [162] showed the observed $m_{e^+e^-}$ distributions down to $m_{e^+e^-} \sim 0$, even though events with $m_{e^+e^-} < 140$ MeV (NA31), $m_{e^+e^-} < 165$ MeV (NA48) were rejected when extracting upper bounds on $\text{Br}(K_S^0 \to \pi^0 e^+e^-)$. In particular, the $m_{e^+e^-}$ distribution in Fig. 3 of [162] shows 2 events within the window of 10 MeV $< m_{e^+e^-} <$ 25 MeV, which could in principle be compatible with an axionic signal from K_S^0 decays with a branching ratio of $\text{Br}(K_S^0 \to \pi^0 a) \sim (2\text{–}3)\times 10^{-7}$. More conservatively, one could instead infer an upper bound of $\text{Br}(K_S^0 \to \pi^0 a) \lesssim 0.8\times 10^{-6}$. For the scenario with $g_8 \gg g_8'$, this would then translate into an upper bound on the axion isoscalar mixing angles of $\theta_{a\eta_{ud}} \lesssim 2\times 10^{-3}$, which is ~3.6 times weaker than the bound on $\theta_{a\eta_{ud}}$ from $K^+ \to \pi^+ a$. In the alternative scenario with $g_8' \gg g_8$, and considering the limiting case of $g_8 \to 0$ [cf. (78)], this would then result in an upper bound on the axion isoscalar mixing angles of $\theta_{a\eta_s} \lesssim 2\times 10^{-2}$, which is comparable with the bound on $\theta_{a\eta_s}$ from $K^+ \to \pi^+ a$.

However, without a proper reinterpretation of the data in [162] by the NA48 Collaboration itself, we cannot have confidence that these inferred limits are accurate; therefore, we refrain from displaying them in Fig. 5. Instead, in Fig. 5, we display the hypothetical reach of $K_S^0 \to \pi^0 a$ to the axion isoscalar mixing angles, assuming an experimental sensitivity[16] to branching ratios $\text{Br}(K_S^0 \to \pi^0 a) \gtrsim 10^{-8}$, under both octet-enhancement scenarios in χPT. Since there is a non-negligible contribution from $\theta_{a\pi}$ in the scenario with $g_8' \gg g_8$, we have chosen the relative sign between $\theta_{a\pi}$ and $\theta_{a\eta_s}$ that yields the most conservative reach in the parameter space of Fig. 5 [cf. (78)].

C. K_L^0 decays

1. CP-violating axio-hadronic K_L^0 decays

Direct CP violation in the neutral kaon system causes K_L^0 to inherit the axio-hadronic decay modes of K_S^0. The resulting branching ratios can be trivially obtained by accounting for $K_L^0 - K_S^0$ mixing, parametrized by the parameter $\epsilon_K \simeq 2.23\times 10^{-3}$,

$$\begin{aligned}\text{Br}(K_L^0 \to \pi^0 a) &= \epsilon_K^2\frac{\Gamma_{K_S}}{\Gamma_{K_L}}\text{Br}(K_S^0 \to \pi^0 a), \\ &\approx 2.8\times 10^{-3}\text{Br}(K_S^0 \to \pi^0 a). \end{aligned} \quad (79)$$

In particular, for the two octet-enhancement scenarios in χPT considered in Sec. V B, we have

$$\text{Br}(K_L^0 \to \pi^0 a)|_{\text{octet enh}} \approx 2\times 10^{-10}\left|\frac{\theta_{a\eta_{ud}}}{5\times 10^{-4}}\right|^2 \quad (80)$$

[16]This choice of branching ratio sensitivity benchmark of 10^{-8} is intended to facilitate comparison between different axionic kaon decay modes and is not informed by any experimental sensitivity projections.

and

$$\mathrm{Br}(K_L^0 \to \pi^0 a)|_{27\text{-plet}} \approx 2 \times 10^{-11} \left| \frac{\theta_{a\eta_s} - 11\theta_{a\pi}}{2 \times 10^{-3}} \right|^2. \quad (81)$$

An upper bound on $K_L^0 \to \pi^0 a$ can be inferred from a search for light Higgs bosons in the final state $K_L^0 \to \pi^0 (h \to e^+e^-)$ performed by CERN's SPS NA31 experiment in 1990 [163]. Assuming that this analysis' efficiency to promptly decaying axions is comparable to that of much longer lived Higgses of mass ∼17 MeV, the bound on the axionic decay would be $\mathrm{Br}(K_L^0 \to \pi^0 (a \to e^+e^-)) \lesssim (1\text{–}2) \times 10^{-8}$. The resulting constraints on the axion isoscalar mixing angles of $\theta_{a\eta_{ud}} \lesssim (3.5\text{–}5) \times 10^{-3}$ (for $g_8' \to 0$) and $\theta_{a\eta_s} \lesssim (4.5\text{–}6.4) \times 10^{-2}$ (for $g_8 \to 0$) are not competitive with limits from $K^+ \to \pi^+ a$ (see Fig. 5).

2. CP-conserving axio-hadronic K_L^0 decays

The CP-conserving axio-hadronic decays of the CP-odd neutral kaon can be estimated via an analogous prescription as the one used in Secs. V A 2 and V B. For specificity, we consider the final state with charged pions, and obtain the contributions to $\mathcal{A}(K_L^0 \to \pi^+\pi^-\varphi^*)$, $\varphi = \pi^0, \eta_{ud}, \eta_s$, from operators (56a), (56b), and (57). Putting K_L^0, π^+, and π^- on shell, we have

$$\mathcal{A}(K_L^0 \to \pi^+\pi^-\pi^{0*}) = \frac{(g_8 + g_8' + 2g_{27})}{3}\frac{m_K^2}{f_\pi^2} - \frac{(g_8 + 4g_8' + 11g_{27})}{3}\frac{m_\pi^2}{f_\pi^2} + \frac{(g_8 + g_8' + 11g_{27})}{3}\frac{p_{\pi^0}^2}{f_\pi^2} + \left(g_8 + g_8' - \frac{5}{2}g_{27}\right)\frac{m_\pi^2 Y}{f_\pi^2}, \quad (82a)$$

$$\mathcal{A}(K_L^0 \to \pi^+\pi^-\eta_{ud}^*) = -\frac{(3g_8 + g_8' - 4g_{27})}{3}\frac{m_K^2}{f_\pi^2} + \frac{(2g_8 + 4g_8' - 3g_{27})}{3}\frac{m_\pi^2}{f_\pi^2} + \frac{(g_8 - g_8' - g_{27})}{3}\frac{p_{\eta_{ud}}^2}{f_\pi^2} - \left(g_8' + \frac{1}{2}g_{27}\right)\frac{m_\pi^2 Y}{f_\pi^2}, \quad (82b)$$

$$\mathcal{A}(K_L^0 \to \pi^+\pi^-\eta_s^*) = \frac{\sqrt{2}}{3}(g_8 - g_8')\frac{m_K^2}{f_\pi^2} + \frac{\sqrt{2}}{3}(4g_8' - g_{27})\frac{m_\pi^2}{f_\pi^2} - \frac{\sqrt{2}}{3}(g_8 + g_8' - g_{27})\frac{p_{\eta_s}^2}{f_\pi^2} + \sqrt{2}\left(g_8 - g_8' - \frac{3}{2}g_{27}\right)\frac{m_\pi^2 Y}{f_\pi^2}, \quad (82c)$$

where the Dalitz plot variable Y has been defined in (62).

Furthermore, an additional effect contributing to $\mathcal{A}(K_L^0 \to \pi\pi a)$ must be taken into account, namely, kinetic mixing between K_L^0 and the neutral pseudoscalar mesons induced by operators O_8 and O_{27},

$$\mathcal{L}_{\chi\mathrm{PT}}^{(\Delta S=1)} \supset -2(g_8 + 2g_{27})\partial_\mu K_L^0 \partial^\mu \pi^0 + 2(g_8 - 2g_{27})\partial_\mu K_L^0 (\partial^\mu \eta_{ud} + \sqrt{2}\partial^\mu \eta_s). \quad (83)$$

In particular, accounting for $K_L^0 - \pi^0$ mixing is crucial in order to obtain the correct dependence of the SM amplitude $\mathcal{A}(K_L^0 \to \pi^+\pi^-\pi^0)$ on g_8 and g_{27}; see (61). Similarly, the contribution to the axionic amplitude $\mathcal{A}(K_L^0 \to \pi\pi a)$ stemming from $K_L^0 - \eta^{(\prime)}$ mixing becomes important in the scenario with $g_8 \gg g_8'$ when $|\theta_{a\eta_{ud}}|$, $|\theta_{a\eta_s}| \lesssim \mathcal{O}(10^{-4})$. It can be straightforwardly obtained by reweighting $\mathcal{A}_{\eta^{(\prime)} \to \pi\pi a}$ in (53),

$$\mathcal{A}(K_L^0 \to \eta^{(\prime)*} \to \pi\pi a) = \frac{C_{K_L^0}}{C_{\eta^{(\prime)}}} \mathcal{A}(\eta^{(\prime)} \to \pi\pi a)|_{p_{\eta^{(\prime)}} \to p_{K_L^0}}, \quad (84)$$

where

$$C_{K_L^0} \equiv 2(g_8 - 2g_{27})\langle \eta_{ud} + \sqrt{2}\eta_s | \left[\frac{m_{K_L^0}^2}{m_\eta^2 - m_{K_L^0}^2} C_\eta |\eta\rangle + \frac{m_{K_L^0}^2}{m_{\eta'}^2 - m_{K_L^0}^2} C_{\eta'} |\eta'\rangle \right] \approx 0.02(g_8 - 2g_{27}), \quad (85)$$

and we have used (37) and (54) in obtaining the approximate equality in (85).

Unfortunately, the amplitude in (84) is subject to the same destructive interference effects, and therefore the same large uncertainties, as $\mathcal{A}(\eta^{(\prime)} \to \pi\pi a)$ estimated in Sec. IV B. In particular, for the region of parameter space where (84) becomes important, these uncertainties make the estimation of $\mathrm{Br}(K_L^0 \to \pi\pi a)$ unreliable. Nonetheless, for the sake of illustration, we will include the effects of $K_L^0 - \eta^{(\prime)}$ mixing in our estimations below by benchmarking the RχT parameters entering in (84) to $m_{a_0} = m_{f_0} = 980$ MeV, $\Gamma_{a_0} = 50$ MeV, $\Gamma_{f_0} = 100$ MeV, and $\widehat{c}_d = \widehat{c}_m = 1$.

The total amplitude $\mathcal{A}(K_L^0 \to \pi^+\pi^- a)$ is then given by the sum of (84) and (82a), (82b), and (82c) reweighted by axion-meson mixing angles,

$$\mathcal{A}(K_L^0 \to \pi^+\pi^- a) = \mathcal{A}(K_L^0 \to \eta^{(\prime)*} \to \pi\pi a) + \theta_{a\pi}\mathcal{A}(K_L^0 \to \pi^+\pi^-\pi^{0*})|_{p_{\pi^0}^2 = m_a^2} + \theta_{a\eta_{ud}}\mathcal{A}(K_L^0 \to \pi^+\pi^-\eta_{ud}^*)|_{p_{\eta_{ud}}^2 = m_a^2} + \theta_{a\eta_s}\mathcal{A}(K_L^0 \to \pi^+\pi^-\eta_s^*)|_{p_{\eta_s}^2 = m_a^2}. \quad (86)$$

Note that $\mathcal{A}(K_L^0 \to \pi^+\pi^- a)$ is octet enhanced in both scenarios, and therefore we can neglect the contributions from g_8' and g_{27} when $g_8 \gg g_8'$, and likewise neglect the contributions from g_8 and g_{27} when $g_8' \gg g_8$. Despite this simplification, obtaining the dependence of $\mathrm{Br}(K_L^0 \to \pi^+\pi^- a)$ on the axion-meson mixing angles still involves nontrivial integration of the differential decay width over the three-body final state phase space. We performed this integration numerically for both octet-enhancement scenarios under the assumptions stated above, and using (61) for normalization, obtained

$$\begin{aligned}\mathrm{Br}(K_L^0 \to \pi^+\pi^- a)|_{g_8 \gg g_8'} &\approx 3.54 \times 10^{-8} \\ &+ 10^{-4} \times (3.83\theta_{a\pi} - 7.42\theta_{a\eta_{ud}} + 5.715\theta_{a\eta_s}) \\ &+ 1.18\theta_{a\pi}^2 + 3.92\theta_{a\eta_{ud}}^2 + 2.60\theta_{a\eta_s}^2 \\ &+ \theta_{a\pi}(-4.125\theta_{a\eta_{ud}} + 3.51\theta_{a\eta_s}) - 6.14\theta_{a\eta_{ud}}\theta_{a\eta_s} \end{aligned} \quad (87)$$

and

$$\mathrm{Br}(K_L^0 \to \pi^+\pi^- a)|_{g_8' \gg g_8} \approx 1.49(\theta_{a\pi} + \theta_{a\eta_{ud}} + \sqrt{2}\theta_{a\eta_s})^2. \quad (88)$$

We remark that the amplitude $\mathcal{A}(K_L^0 \to \pi^0\pi^0 a)$ is simply related to $\mathcal{A}(K_L^0 \to \pi^+\pi^- a)$ by isospin symmetry, which results in

$$\mathrm{Br}(K_L^0 \to \pi^0\pi^0 a) = \frac{1}{2}\mathrm{Br}(K_L^0 \to \pi^+\pi^- a). \quad (89)$$

In Fig. 5, we show the hypothetical reach of $K_L^0 \to \pi^+\pi^- a$ to the axion isoscalar mixing angles assuming an experimental sensitivity[17] to branching ratios $\mathrm{Br}(K_L^0 \to \pi^+\pi^- a) \gtrsim 10^{-8}$, under both octet-enhancement scenarios in χPT. Since the contribution from $\theta_{a\pi}$ is nonnegligible for the chosen branching ratio sensitivity benchmark of 10^{-8}, the contours in Fig. 5 implicitly assume the relative sign between $\theta_{a\pi}$ and $\theta_{a\eta_{ud}}$ that yields the most conservative reach.

It is worth mentioning an exception to our estimations of $\mathcal{A}(K_L^0 \to \pi^+\pi^- a)$ presented in this section. Besides the two limiting cases we have been considering of $g_8 \gg g_8'$ and $g_8 \ll g_8'$, there is also the possibility that g_8 and g_8' have comparable magnitudes. In this case, there would be nonnegligible interference between the amplitudes for $K_L^0 \to \pi^+\pi^- a$ originating from operators O_8 and O_8', which could substantially modify the dependence of $\mathrm{Br}(K_L^0 \to \pi^+\pi^- a)$ on the axion-meson mixing angles.

[17]This choice of branching ratio sensitivity benchmark of 10^{-8} is intended to facilitate comparison between different axionic kaon decay modes and is not informed by any experimental sensitivity projections.

Despite the assumptions, simplifications, and uncertainties of our estimations, the $K_L^0 \to \pi^+\pi^- a$ contours in Fig. 5 offer a compelling motivation for upcoming kaon experiments to search for an $m_{e^+e^-} \sim 17$ MeV resonance in $K_L^0 \to \pi\pi e^+e^-$ final states.[18] If these searches could achieve sensitivities down to branching ratios of $\mathcal{O}(10^{-8})$, they could almost fully exclude the parameter space favored by (or verify the QCD axion explanation of) the ^{8}Be, ^{4}He, and KTeV anomalies.

3. Dielectronic K_L^0 decays

The last rare kaon decay we shall consider is $K_L^0 \to e^+e^-$, whose amplitude can receive a potentially non-negligible contribution from $K_L^0 - \eta^{(\prime)} - a$ mixing. Indeed, using (83) and momentarily neglecting the SM contribution to the amplitude, it follows that the $K_L^0 \to e^+e^-$ rate induced by $K_L^0 - \eta^{(\prime)} - a$ mixing would be

$$\begin{aligned}&\mathrm{Br}(K_L^0 \to e^+e^-)|_{\mathcal{A}_{\mathrm{SM}} \to 0} \\ &\simeq \frac{1}{\Gamma_{K_L^0}} \frac{m_{K_L^0}}{8\pi} \left| \frac{q_{\mathrm{PQ}}^e m_e}{f_a} (2g_8 - 4g_{27})(\theta_{a\eta_{ud}} + \sqrt{2}\theta_{a\eta_s}) \right|^2 \\ &\simeq 0.9 \times 10^{-11} \left| \frac{g_8 - 2g_{27}}{g_8 + g_8'} \right|^2 (q_{\mathrm{PQ}}^e)^2 \left(\frac{\theta_{a\eta_{ud}} + \sqrt{2}\theta_{a\eta_s}}{10^{-3}} \right)^2. \end{aligned} \quad (90)$$

The estimate above should be contrasted with the observed $K_L^0 \to e^+e^-$ rate [167], as well as the range of SM predictions [168–170],

$$\mathrm{Br}(K_L^0 \to e^+e^-)|_{\mathrm{exp}} = (0.87^{+0.57}_{-0.41}) \times 10^{-11}, \quad (91)$$

$$\mathrm{Br}(K_L^0 \to e^+e^-)|_{\mathrm{SM}} \sim (0.3\text{–}0.9) \times 10^{-11}. \quad (92)$$

From (90) and (91), we can extract a nontrivial upper bound on the axion isoscalar mixing angles in the octet-enhancement scenario with $g_8 \gg g_8'$ (shown in Fig. 5),

$$|\theta_{a\eta_{ud}} + \sqrt{2}\theta_{a\eta_s}|\Big|_{g_8 \gg g_8'} \lesssim 0.5 \times 10^{-2} \left(\frac{1/3}{|q_{\mathrm{PQ}}^e|} \right). \quad (93)$$

For $|q_{\mathrm{PQ}}^e(\theta_{a\eta_{ud}} + \sqrt{2}\theta_{a\eta_s})| \lesssim 10^{-3}$, however, the SM contribution to the amplitude cannot be neglected; in this case, the estimation in (90) is not accurate. Indeed, for a significant part of the parameter space favored by the ^{8}Be and ^{4}He anomalies, the axionic contribution to $K_L^0 \to e^+e^-$ is subdominant to that of the SM, and in fact it is negligible in the octet-enhancement scenario with $g_8 \ll g_8'$. A tantalizing possibility remains, however, that once measurements and theoretical predictions are improved over (91)

[18]Dedicated reanalyses of existing data in $K_L^0 \to \pi\pi e^+e^-$ final states could also be potentially sensitive to the axionic signal. See, e.g., [164–166].

and (92), a piophobic QCD axion signal could appear in this channel as an excess over the SM expectation.

VI. SUMMARY AND DISCUSSION

The PQ mechanism was conceived to address a problem intrinsic to the nonperturbative dynamics of QCD. Yet, presently, the prevalent view is that PQ symmetry breaking should take place at scales $f_{\rm PQ} \gtrsim 10^{10}\Lambda_{\rm QCD}$. Why should these two scales be so widely separated? PQ cancellation of the strong CP phase would be much more robust against spoiling effects if $f_{\rm PQ} \sim \Lambda_{\rm QCD}$. This possibility has long been dismissed due to stringent laboratory constraints on the visible QCD axion, in particular on its isovector couplings. More recently, however, we showed in [46] that the $\mathcal{O}(10)$ MeV mass range for the QCD axion remains compatible with all existing experimental constraints if the QCD axion (i) couples dominantly to the first generation of SM fermions; (ii) is short lived, decaying with lifetimes $\lesssim 4 \times 10^{-14}$ s to e^+e^-; and (iii) is piophobic, i.e., has suppressed isovector couplings due to an accidental cancelation of its mixing with the neutral pion, $\theta_{a\pi} \lesssim 10^{-4}$. These conditions require nontrivial UV completions, but so does *any* viable QCD axion model, whether "heavy" and short lived or ultralight and cosmologically long lived.

While this possibility forgoes the attractive feature of explaining the particle nature of dark matter, it offers a single, consistent explanation for a few persistent experimental anomalies: the observed rate for $\pi^0 \to e^+e^-$, and the "bumplike" excesses in the e^+e^- spectra of (predominantly) isoscalar magnetic transitions of excited ^{8}Be and ^{4}He nuclei. Unsurprisingly, such signals have long been predicted as smoking gun signatures of the QCD axion.

In this paper, we estimated the axionic emission rates of the relevant ^{8}Be and ^{4}He transitions, taking nuclear and χPT uncertainties into account, and showed that the piophobic QCD axion provides a natural and compelling explanation of the observed data for these two nuclei with quite distinct properties. We also considered in detail potential axionic signals in rare decays of the η, η', $K^\pm$, and $K^0_{S,L}$ mesons. The (often ignored) hadronic and χPT uncertainties involved in estimations of these rare meson decays impede accurate predictions of axio-hadronic signals; nonetheless, the ranges we have obtained for several of the processes investigated can be probed in the near future in a variety of experimental programs, including η/η' and kaon factories.

ACKNOWLEDGMENTS

I am grateful to Anna Hayes and Gerry Hale for explanations of electromagnetic transitions of ^{8}Be and ^{4}He nuclei. I also thank Maxim Pospelov for discussions on the experimental sensitivity of the COSY-WASA analysis to axionic η decays, and Corrado Gatto for discussions about the REDTOP experiment. This work was supported by an Early Career Research award from Los Alamos National Laboratory's LDRD program and by the DOE Office of Science High Energy Physics under Contract No. DE-AC52-06NA25396.

[1] J. Jaeckel and A. Ringwald, The low-energy frontier of particle physics, Annu. Rev. Nucl. Part. Sci. **60**, 405 (2010).
[2] J. L. Hewett *et al.*, Fundamental physics at the intensity frontier,(2012), https://dx.doi.org.10.2172/1042577.
[3] J. Alexander *et al.*, Dark sectors 2016 workshop: Community report, arXiv:1608.08632.
[4] N. Arkani-Hamed, D. P. Finkbeiner, T. R. Slatyer, and N. Weiner, A theory of dark matter, Phys. Rev. D **79**, 015014 (2009).
[5] B. Batell, M. Pospelov, and A. Ritz, Probing a secluded U(1) at B-factories, Phys. Rev. D **79**, 115008 (2009).
[6] R. Essig, P. Schuster, and N. Toro, Probing dark forces and light hidden sectors at low-energy e + e− colliders, Phys. Rev. D **80**, 015003 (2009).
[7] J. D. Bjorken, R. Essig, P. Schuster, and N. Toro, New fixed-target experiments to search for dark gauge forces, Phys. Rev. D **80**, 075018 (2009).
[8] B. Batell, M. Pospelov, and A. Ritz, Exploring portals to a hidden sector through fixed targets, Phys. Rev. D **80**, 095024 (2009).
[9] P. deNiverville, M. Pospelov, and A. Ritz, Observing a light dark matter beam with neutrino experiments, Phys. Rev. D **84**, 075020 (2011).
[10] B. A. Dobrescu and C. Frugiuele, GeV-scale dark matter: Production at the main injector, J. High Energy Phys. 02 (2015) 019.
[11] C. Frugiuele, Probing sub-GeV dark sectors via high energy proton beams at LBNF/DUNE and MiniBooNE, Phys. Rev. D **96**, 015029 (2017).
[12] L. Buonocore, C. Frugiuele, and P. deNiverville, Hunt for sub-GeV dark matter at neutrino facilities: A survey of past and present experiments, Phys. Rev. D **102**, 035006 (2020).
[13] Kickoff Meeting of the RF6 SNOWMASS Working Group, Dark Sectors at High Intensities, https://indico.fnal.gov/event/44819/
[14] R. D. Peccei and H. R. Quinn, *CP* Conservation in the Presence of Instantons, Phys. Rev. Lett. **38**, 1440 (1977).
[15] R. D. Peccei and H. R. Quinn, Constraints imposed by *CP* conservation in the presence of instantons, Phys. Rev. D **16**, 1791 (1977).

[16] S. Weinberg, A New Light Boson?, Phys. Rev. Lett. **40**, 223 (1978).
[17] F. Wilczek, Problem of Strong p and t Invariance in the Presence of Instantons, Phys. Rev. Lett. **40**, 279 (1978).
[18] J. E. Kim, Weak Interaction Singlet and Strong *CP* Invariance, Phys. Rev. Lett. **43**, 103 (1979).
[19] M. A. Shifman, A. I. Vainshtein, and V. I. Zakharov, Can confinement ensure natural *CP* invariance of strong interactions?, Nucl. Phys. **B166**, 493 (1980).
[20] M. Dine, W. Fischler, and M. Srednicki, A simple solution to the strong *CP* problem with a harmless axion, Phys. Lett. **104B**, 199 (1981).
[21] J. Preskill, M. B. Wise, and F. Wilczek, Cosmology of the invisible axion, Phys. Lett. **120B**, 127 (1983).
[22] L. F. Abbott and P. Sikivie, A cosmological bound on the invisible axion, Phys. Lett. **120B**, 133 (1983).
[23] M. Dine and W. Fischler, The not so harmless axion, Phys. Lett. **120B**, 137 (1983).
[24] C. E. Aalseth *et al.*, The CERN axion solar telescope (CAST), Nucl. Phys. B, Proc. Suppl. **110**, 85 (2002).
[25] S. J. Asztalos *et al.* (ADMX Collaboration), A SQUID-Based Microwave Cavity Search for Dark-Matter Axions, Phys. Rev. Lett. **104**, 041301 (2010).
[26] D. Budker, P. W. Graham, M. Ledbetter, S. Rajendran, and A. Sushkov, Proposal for a Cosmic Axion Spin Precession Experiment (CASPEr), Phys. Rev. X **4**, 021030 (2014).
[27] S. K. Lamoreaux, K. A. van Bibber, K. W. Lehnert, and G. Carosi, Analysis of single-photon and linear amplifier detectors for microwave cavity dark matter axion searches, Phys. Rev. D **88**, 035020 (2013).
[28] E. Armengaud *et al.*, Conceptual design of the international axion observatory (IAXO), J. Instrum. **9**, T05002 (2014).
[29] A. Arvanitaki and A. A. Geraci, Resonantly Detecting Axion-Mediated Forces with Nuclear Magnetic Resonance, Phys. Rev. Lett. **113**, 161801 (2014).
[30] G. Rybka, A. Wagner, A. Brill, K. Ramos, R. Percival, and K. Patel, Search for dark matter axions with the Orpheus experiment, Phys. Rev. D **91**, 011701 (2015).
[31] P. W. Graham, I. G. Irastorza, S. K. Lamoreaux, A. Lindner, and K. A. van Bibber, Experimental searches for the axion and axion-like particles, Annu. Rev. Nucl. Part. Sci. **65**, 485 (2015).
[32] Y. Kahn, B. R. Safdi, and J. Thaler, Broadband and Resonant Approaches to Axion Dark Matter Detection, Phys. Rev. Lett. **117**, 141801 (2016).
[33] M. Baryakhtar, J. Huang, and R. Lasenby, Axion and hidden photon dark matter detection with multilayer optical haloscopes, Phys. Rev. D **98**, 035006 (2018).
[34] I. G. Irastorza and J. Redondo, New experimental approaches in the search for axion-like particles, Prog. Part. Nucl. Phys. **102**, 89 (2018).
[35] P. Brun *et al.* (MADMAX Collaboration), A new experimental approach to probe QCD axion dark matter in the mass range above 40 μeV, Eur. Phys. J. C **79**, 186 (2019).
[36] W. A. Bardeen and S. H. H. Tye, Current algebra applied to Properties of the light Higgs boson, Phys. Lett. **74B**, 229 (1978).
[37] R. Holman, S. D. H. Hsu, T. W. Kephart, E. W. Kolb, R. Watkins, and L. M. Widrow, Solutions to the strong *CP* problem in a world with gravity, Phys. Lett. B **282**, 132 (1992).
[38] M. Kamionkowski and J. March-Russell, Planck scale physics and the Peccei-Quinn mechanism, Phys. Lett. B **282**, 137 (1992).
[39] S. M. Barr and D. Seckel, Planck scale corrections to axion models, Phys. Rev. D **46**, 539 (1992).
[40] S. Ghigna, M. Lusignoli, and M. Roncadelli, Instability of the invisible axion, Phys. Lett. B **283**, 278 (1992).
[41] R. Kallosh, A. D. Linde, D. A. Linde, and L. Susskind, Gravity and global symmetries, Phys. Rev. D **52**, 912 (1995).
[42] S. Gori, G. Perez, and K. Tobioka, KOTO vs. NA62 dark scalar searches, J. High Energy Phys. 08 (2020) 110.
[43] A. J. Krasznahorkay *et al.*, Observation of Anomalous Internal Pair Creation in Be8: A Possible Indication of a Light, Neutral Boson, Phys. Rev. Lett. **116**, 042501 (2016).
[44] A. J. Krasznahorkay *et al.*, New evidence supporting the existence of the hypothetic X17 particle, arXiv:1910.10459.
[45] E. Abouzaid *et al.* (KTeV Collaboration), Measurement of the rare decay $\pi^0 \to e^+e^-$, Phys. Rev. D **75**, 012004 (2007).
[46] D. S. M. Alves and N. Weiner, A viable QCD axion in the MeV mass range, J. High Energy Phys. 07 (2018) 092.
[47] D. Aloni, Y. Soreq, and M. Williams, Coupling QCD-Scale Axionlike Particles to Gluons, Phys. Rev. Lett. **123**, 031803 (2019).
[48] A. E. Dorokhov and M. A. Ivanov, Rare decay pi0− > e + e−: Theory confronts KTeV data, Phys. Rev. D **75**, 114007 (2007).
[49] A. E. Dorokhov, E. A. Kuraev, Yu. M. Bystritskiy, and M. Secansky, QED radiative corrections to the decay pi0− > e + e−, Eur. Phys. J. C **55**, 193 (2008).
[50] P. Vasko and J. Novotny, Two-loop QED radiative corrections to the decay pi0− > e + e−: The virtual corrections and soft-photon bremsstrahlung, J. High Energy Phys. 10 (2011) 122.
[51] T. Husek, K. Kampf, and J. Novotný, Rare decay $\pi^0 \to e^+e^-$: On corrections beyond the leading order, Eur. Phys. J. C **74**, 3010 (2014).
[52] D. V. Kirpichnikov, V. E. Lyubovitskij, and A. S. Zhevlakov, Implication of hidden sub-GeV bosons for the $(g-2)_\mu$, ^{8}Be-^{4}He anomaly, proton charge radius, EDM of fermions, and dark axion portal, Phys. Rev. D **102**, 095024 (2020).
[53] J. L. Feng, B. Fornal, I. Galon, S. Gardner, J. Smolinsky, T. M. P. Tait, and P. Tanedo, Protophobic Fifth-Force Interpretation of the Observed Anomaly in ^{8}Be Nuclear Transitions, Phys. Rev. Lett. **117**, 071803 (2016).
[54] J. L. Feng, B. Fornal, I. Galon, S. Gardner, J. Smolinsky, T. M. P. Tait, and P. Tanedo, Particle physics models for the 17 MeV anomaly in beryllium nuclear decays, Phys. Rev. D **95**, 035017 (2017).
[55] J. L. Feng, T. M. P. Tait, and C. B. Verhaaren, Dynamical evidence for a fifth force explanation of the ATOMKI nuclear anomalies, Phys. Rev. D **102**, 036016 (2020).

[56] X. Zhang and G. A. Miller, Can a protophobic vector boson explain the ATOMKI anomaly?, Phys. Lett. B **813**, 136061 (2021).

[57] Y. Kahn, G. Krnjaic, S. Mishra-Sharma, and T. M. P. Tait, Light weakly coupled axial forces: Models, constraints, and projections, J. High Energy Phys. 05 (2017) 002.

[58] J. Kozaczuk, D. E. Morrissey, and S. R. Stroberg, Light axial vector bosons, nuclear transitions, and the ^{8}Be anomaly, Phys. Rev. D **95**, 115024 (2017).

[59] S. B. Treiman and F. Wilczek, Axion emission in decay of excited nuclear states, Phys. Lett. **74B**, 381 (1978).

[60] T. W. Donnelly, S. J. Freedman, R. S. Lytel, R. D. Peccei, and M. Schwartz, Do axions exist?, Phys. Rev. D **18**, 1607 (1978).

[61] A. Barroso and N. C. Mukhopadhyay, Nuclear axion decay, Phys. Rev. C **24**, 2382 (1981).

[62] I. Antoniadis and T. N. Truong, Lower bound for branching ratio of $K^+ \to \pi^+$ axion and nonexistence of Peccei-Quinn axion, Phys. Lett. **109B**, 67 (1982).

[63] W. A. Bardeen, R. D. Peccei, and T. Yanagida, Constraints on variant axion models, Nucl. Phys. **B279**, 401 (1987).

[64] L. M. Krauss and M. B. Wise, Constraints on shortlived axions from the decay $\pi^+ \to e^+e^-e^+$ neutrino, Phys. Lett. B **176**, 483 (1986).

[65] M. Davier, Searches for new particles, in *Proceedings, 23RD International Conference on High Energy Physics, Berkeley, CA* (Berkeley National Laboratory, Berkeley,1986).

[66] L. M. Krauss and D. J. Nash, A viable weak interaction axion?, Phys. Lett. B **202**, 560 (1988).

[67] A. Anastasi *et al.*, Limit on the production of a low-mass vector boson in $e^+e^- \to U\gamma$, $U \to e^+e^-$ with the KLOE experiment, Phys. Lett. B **750**, 633 (2015).

[68] D. Banerjee *et al.* (NA64 Collaboration), Improved limits on a hypothetical X(16.7) boson and a dark photon decaying into e^+e^- pairs, Phys. Rev. D **101**, 071101 (2020).

[69] E. Depero *et al.*, Hunting down the X17 boson at the CERN SPS, Eur. Phys. J. C **80**, 1159 (2020).

[70] Z. Fodor, C. Hoelbling, S. Krieg, L. Lellouch, Th. Lippert, A. Portelli, A. Sastre, K. K. Szabo, and L. Varnhorst, Up and Down Quark Masses and Corrections to Dashen's Theorem from Lattice QCD and Quenched QED, Phys. Rev. Lett. **117**, 082001 (2016).

[71] R. L. Jaffe and A. Manohar, The G(1) problem: Fact and fantasy on the spin of the proton, Nucl. Phys. **B337**, 509 (1990).

[72] M. J. Savage and J. Walden, SU(3) breaking in neutral current axial matrix elements and the spin content of the nucleon, Phys. Rev. D **55**, 5376 (1997).

[73] M. Karliner and H. J. Lipkin, Nucleon spin with and without hyperon data: A new tool for analysis, Phys. Lett. B **461**, 280 (1999).

[74] G. K. Mallot, The Spin structure of the nucleon, Int. J. Mod. Phys. A **15**, 521 (2000).

[75] E. Leader, A. V. Sidorov, and D. B. Stamenov, On the sensitivity of the polarized parton densities to flavor SU(3) symmetry breaking, Phys. Lett. B **488**, 283 (2000).

[76] H.-Y. Cheng and C.-W. Chiang, Revisiting scalar and pseudoscalar couplings with nucleons, J. High Energy Phys. 07 (2012) 009.

[77] G. S. Bali *et al.* (QCDSF Collaboration), Strangeness Contribution to the Proton Spin from Lattice QCD, Phys. Rev. Lett. **108**, 222001 (2012).

[78] M. Engelhardt, Strange quark contributions to nucleon mass and spin from lattice QCD, Phys. Rev. D **86**, 114510 (2012).

[79] A. Abdel-Rehim, C. Alexandrou, M. Constantinou, V. Drach, K. Hadjiyiannakou, K. Jansen, G. Koutsou, and A. Vaquero, Disconnected quark loop contributions to nucleon observables in lattice QCD, Phys. Rev. D **89**, 034501 (2014).

[80] T. Bhattacharya, R. Gupta, and B. Yoon, Disconnected quark loop contributions to nucleon structure, *Proc. Sci.*, LATTICE2014 (2014) 141.

[81] A. Abdel-Rehim *et al.*, Nucleon and pion structure with lattice QCD simulations at physical value of the pion mass, Phys. Rev. D **92**, 114513 (2015); , Erratum, Phys. Rev. D **93**, 039904 (2016).

[82] A. Abdel-Rehim, C. Alexandrou, M. Constantinou, K. Hadjiyiannakou, K. Jansen, C. Kallidonis, G. Koutsou, and A. V. Avilés-Casco, Disconnected quark loop contributions to nucleon observables using $N_f = 2$ twisted clover fermions at the physical value of the light quark mass, *Proc. Sci.*, LATTICE2015 (2016) 136.

[83] J. Green, N. Hasan, S. Meinel, M. Engelhardt, S. Krieg, J. Laeuchli, J. Negele, K. Orginos, A. Pochinsky, and S. Syritsyn, Up, down, and strange nucleon axial form factors from lattice QCD, Phys. Rev. D **95**, 114502 (2017).

[84] F. P. Calaprice, R. W. Dunford, R. T. Kouzes, M. Miller, A. Hallin, M. Schneider, and D. Schreiber, Search for axion emission in the decay of excited states of C-12, Phys. Rev. D **20**, 2708 (1979).

[85] M. J. Savage, R. D. Mckeown, B. W. Filippone, and L. W. Mitchell, Search for a Shortlived Neutral Particle Produced in Nuclear Decay, Phys. Rev. Lett. **57**, 178 (1986).

[86] A. L. Hallin, F. P. Calaprice, R. W. Dunford, and A. B. Mcdonald, Restrictions on a 1.7-MeV Axion From Nuclear Pair Transitions, Phys. Rev. Lett. **57**, 2105 (1986).

[87] F. W. N. De Boer, K. Abrahams, A. Balanda, H. Bokemeyer, R. Van Dantzig, J. F. W. Jansen, B. Kotlinski, M. J. A. De Voigt, and J. Van Klinken, Search for shortlived axions in a nuclear isoscalar transition, Phys. Lett. B **180**, 4 (1986).

[88] A. L. Hallin, F. P. Calaprice, R. W. Dunford, A. B. Mcdonald, and G. C. Paulson, Limits on axions from nuclear decays, Nucl. Instrum. Methods Phys. Res., Sect. B **24/25**, 276 (1987).

[89] F. T. Avignone, C. Baktash, W. C. Barker, F. P. Calaprice, R. W. Dunford, W. C. Haxton, D. Kahana, R. T. Kouzes, H. S. Miley, and D. M. Moltz, Search for Axions from the 1115-kev transition of ^{65}Cu, Phys. Rev. D **37**, 618 (1988).

[90] M. J. Savage, B. W. Filippone, and L. W. Mitchell, New limits on light scalar and pseudoscalar particles produced in nuclear decay, Phys. Rev. D **37**, 1134 (1988).

[91] V. M. Datar, S. Fortier, S. Gales, E. Hourani, H. Langevin, J. M. Maison, and C. P. Massolo, Search for short lived neutral particle in the 15.1-Mev isovector transition of C-12, Phys. Rev. C **37**, 250 (1988).

[92] S. Freedman, Search for shortlived axions, Nucl. Instrum. Methods Phys. Res., Sect. A **284**, 50 (1989).

[93] T. Asanuma, M. Minowa, T. Tsukamoto, S. Orito, and T. Tsunoda, A search for correlated e + e− pairs in the decay of AM-241, Phys. Lett. B **237**, 588 (1990).

[94] S. Pastore, R. B. Wiringa, Steven C. Pieper, and R. Schiavilla, Quantum Monte Carlo calculations of electromagnetic transitions in ^{8}Be with meson-exchange currents derived from chiral effective field theory, Phys. Rev. C **90**, 024321 (2014).

[95] A. J. Krasznahorkay, M. Csatlós, L. Csige, D. Firak, J. Gulyás, Á. Nagy, N. Sas, J. Timár, T. G. Tornyi, and A. Krasznahorkay, On the $X(17)$ light-particle candidate observed in nuclear transitions, Acta Phys. Pol. B **50**, 675 (2019).

[96] D. R. Tilley, J. H. Kelley, J. L. Godwin, D. J. Millener, J. E. Purcell, C. G. Sheu, and H. R. Weller, Energy levels of light nuclei A = 8,9,10, Nucl. Phys. **A745**, 155 (2004).

[97] G. G. di Cortona, E. Hardy, J. Pardo Vega, and G. Villadoro, The QCD axion, precisely, J. High Energy Phys. 01 (2016) 034.

[98] T. W. Donnelly and R. D. Peccei, Neutral current effects in nuclei, Phys. Rep. **50**, 1 (1979).

[99] X. Zhang and G. A. Miller, Can nuclear physics explain the anomaly observed in the internal pair production in the Beryllium-8 nucleus?, Phys. Lett. B **773**, 159 (2017).

[100] C.-Y. Chen, D. McKeen, and M. Pospelov, New physics via pion capture and simple nuclear reactions, Phys. Rev. D **100**, 095008 (2019).

[101] L. Gan, B. Kubis, E. Passemar, and S. Tulin, Precision tests of fundamental physics with η and η' mesons, arXiv: 2007.00664.

[102] D. J. Mack, Physics and outlook for rare, all-neutral Eta decays, EPJ Web Conf. **73**, 03015 (2014).

[103] D. González, D. León, B. Fabela, and M. I. Pedraza, Detecting physics beyond the standard model with the REDTOP experiment, J. Phys. Conf. Ser. **912**, 012042 (2017).

[104] C. Gatto, B. F. Enriquez, and M. Isabel Pedraza Morales (REDTOP Collaboration), The REDTOP project: Rare eta decays with a TPC for optical photons, *Proc. Sci.*, ICHEP2016 (2016) 812.

[105] G. Agakishiev *et al.* (HADES Collaboration), Searching a dark photon with HADES, Phys. Lett. B **731**, 265 (2014).

[106] M. N. Achasov *et al.* (SND Collaboration), Search for the process $\mathbf{e^+e^-} \to \eta$, Phys. Rev. D **98**, 052007 (2018).

[107] L. G. Landsberg, Electromagnetic decays of light mesons, Phys. Rep. **128**, 301 (1985).

[108] A. E. Dorokhov, M. A. Ivanov, and S. G. Kovalenko, Complete structure dependent analysis of the decay $P- > 1 + 1-$, Phys. Lett. B **677**, 145 (2009).

[109] P. Masjuan and P. Sanchez-Puertas, η and η' decays into lepton pairs, J. High Energy Phys. 08 (2016) 108.

[110] R. Escribano and J.-M. Frere, Study of the eta—eta-prime system in the two mixing angle scheme, J. High Energy Phys. 06 (2005) 029.

[111] G. Landini and E. Meggiolaro, Study of the interactions of the axion with mesons and photons using a chiral effective Lagrangian model, Eur. Phys. J. C **80**, 302 (2020).

[112] J. A. Cronin, Phenomenological model of strong and weak interactions in chiral U(3) × U(3), Phys. Rev. **161**, 1483 (1967).

[113] H. Osborn and D. J. Wallace, Eta—x mixing, eta → 3pi and chiral lagrangians, Nucl. Phys. **B20**, 23 (1970).

[114] J. Gasser and H. Leutwyler, eta → 3pi to one loop, Nucl. Phys. **B250**, 539 (1985).

[115] A. Kupsc, What is interesting in eta and eta-prime meson decays?, AIP Conf. Proc. **950**, 165 (2007).

[116] J. Kambor, C. Wiesendanger, and D. Wyler, Final state interactions and Khuri-Treiman equations in eta → 3pi decays, Nucl. Phys. **B465**, 215 (1996).

[117] B. Borasoy and R. Nissler, Hadronic eta and eta-prime decays, Eur. Phys. J. A **26**, 383 (2005).

[118] A. V. Anisovich and H. Leutwyler, Dispersive analysis of the decay eta → 3pi, Phys. Lett. B **375**, 335 (1996).

[119] J. Bijnens and K. Ghorbani, eta → 3pi at two loops in chiral perturbation theory, J. High Energy Phys. 11 (2007) 030.

[120] P. Guo, I. V. Danilkin, D. Schott, C. Fernández-Ramírez, V. Mathieu, and A. P. Szczepaniak, Three-body final state interaction in eta → 3pi, Phys. Rev. D **92**, 054016 (2015).

[121] P. Guo, I. V. Danilkin, C. Fernández-Ramírez, V. Mathieu, and A. P. Szczepaniak, Three-body final state interaction in eta → 3pi updated, Phys. Lett. B **771**, 497 (2017).

[122] G. Colangelo, S. Lanz, H. Leutwyler, and E. Passemar, Dispersive analysis of $\eta \to 3\pi$, Eur. Phys. J. C **78**, 947 (2018).

[123] P. Herrera-Siklody, Eta and eta-prime hadronic decays in U(L)(3) × U(R)(3) chiral perturbation theory, arXiv:hep-ph/9902446.

[124] B. Borasoy, U.-G. Meissner, and R. Nissler, On the extraction of the quark mass ratio (m(d)- m(u)) / m(s) from Gamma(eta−prime→pi0pi+pi−)/Gamma(eta−prime→etapi+pi−), Phys. Lett. B **643**, 41 (2006).

[125] A. H. Fariborz and J. Schechter, Eta − prime → eta pi pi decay as a probe of a possible lowest lying scalar nonet, Phys. Rev. D **60**, 034002 (1999).

[126] A. M. Abdel-Rehim, D. Black, A. H. Fariborz, and J. Schechter, Effects of light scalar mesons in eta → three pi decay, Phys. Rev. D **67**, 054001 (2003).

[127] G. Ecker, J. Gasser, A. Pich, and E. de Rafael, The role of resonances in chiral perturbation theory, Nucl. Phys. **B321**, 311 (1989).

[128] G. Ecker, J. Gasser, H. Leutwyler, A. Pich, and E. de Rafael, Chiral Lagrangians for massive spin 1 fields, Phys. Lett. B **223**, 425 (1989).

[129] J. A. Oller and E. Oset, Chiral symmetry amplitudes in the S wave isoscalar and isovector channels and the σ, $f_0(980)$, $a_0(980)$ scalar mesons, Nucl. Phys. **A620**, 438 (1997); Erratum, Nucl. Phys. **652**, 407 (1999).

[130] V. Cirigliano, G. Ecker, H. Neufeld, and A. Pich, Meson resonances, large N(c) and chiral symmetry, J. High Energy Phys. 06 (2003) 012.

[131] J. Gasser and H. Leutwyler, Chiral perturbation theory: Expansions in the mass of the strange quark, Nucl. Phys. **B250**, 465 (1985).

[132] A. Pich, Effective Field theory with Nambu-Goldstone modes, *Lecture Notes of the Les Houches Summer School* (Oxford University Press, Oxford, 2020), Vol. 108.

[133] P. A. Zyla *et al.* (Particle Data Group), Review of particle physics, Prog. Theor. Exp. Phys. **2020**, 083C01 (2020).

[134] A. Pich, Colorless mesons in a polychromatic world, in *Phenomenology of large N(c) QCD. Proceedings, Tempe, USA* (World Scientific, Singapore, 2002), pp. 239–258.
[135] M. F. L. Golterman and S. Peris, The 7/11 Rule: An estimate of m(rho)/f(pi), Phys. Rev. D **61**, 034018 (2000).
[136] M. Jamin, J. A. Oller, and A. Pich, S wave K pi scattering in chiral perturbation theory with resonances, Nucl. Phys. **B587**, 331 (2000).
[137] M. Jamin, J. A. Oller, and A. Pich, Strangeness changing scalar form-factors, Nucl. Phys. **B622**, 279 (2002).
[138] F. Ambrosino *et al.* (KLOE Collaboration), Measurement of the branching ratio and search for a *CP* violating asymmetry in the $\eta \to \pi^+\pi^- e^+ e^- (\gamma)$ decay at KLOE, Phys. Lett. B **675**, 283 (2009).
[139] C. Bargholtz *et al.* (CELSIUS/WASA Collaboration), Measurement of the eta → pi + pi − e + e− decay branching ratio, Phys. Lett. B **644**, 299 (2007).
[140] M. Berlowski *et al.* (CELSIUS/WASA Collaboration), Measurement of eta meson decays into lepton-antilepton pairs, Phys. Rev. D **77**, 032004 (2008).
[141] P. Naik *et al.* (CLEO Collaboration), Observation of Eta-Prime Decays to pi+ pi- pi0 and pi+ pi- e+ e-, Phys. Rev. Lett. **102**, 061801 (2009).
[142] M. Ablikim *et al.* (BESIII Collaboration), Measurement of $\eta' \to \pi^+\pi^- e^+ e^-$ and $\eta' \to \pi^+\pi^-\mu^+\mu^-$, Phys. Rev. D **87**, 092011 (2013).
[143] E. C. Gil *et al.* (NA62 Collaboration), The beam and detector of the NA62 experiment at CERN, J. Instrum. **12**, P05025 (2017).
[144] E. Iwai (KOTO Collaboration), Status and prospects of J-PARC KOTO experiment, Nucl. Phys. B, Proc. Suppl. **233**, 279 (2012).
[145] C. W. Bernard, T. Draper, A. Soni, H. D. Politzer, and M. B. Wise, Application of chiral perturbation theory to $K \to 2$ pi decays, Phys. Rev. D **32**, 2343 (1985).
[146] J. Kambor, J. H. Missimer, and D. Wyler, The chiral loop expansion of the nonleptonic weak interactions of mesons, Nucl. Phys. **B346**, 17 (1990).
[147] V. Cirigliano, G. Ecker, H. Neufeld, A. Pich, and J. Portoles, Kaon decays in the standard model, Rev. Mod. Phys. **84**, 399 (2012).
[148] J. M. Gerard and J. Weyers, Trace anomalies and the delta I = 1/2 rule, Phys. Lett. B **503**, 99 (2001).
[149] R. J. Crewther and L. C. Tunstall, $\Delta I = 1/2$ rule for kaon decays derived from QCD infrared fixed point, Phys. Rev. D **91**, 034016 (2015).
[150] A. J. Buras, J.-M. Gérard, and W. A. Bardeen, Large N approach to kaon decays and mixing 28 years later: $\Delta I = 1/2$ rule, $\hat{B}_K$ and ΔM_K, Eur. Phys. J. C **74**, 2871 (2014).
[151] J. Kambor, J. H. Missimer, and D. Wyler, $K \to 2$ pi and $K \to 3$ pi decays in next-to-leading order chiral perturbation theory, Phys. Lett. B **261**, 496 (1991).
[152] J. Bijnens, P. Dhonte, and F. Persson, $K \to 3$ pi decays in chiral perturbation theory, Nucl. Phys. **B648**, 317 (2003).
[153] J. F. Donoghue, E. Golowich, and B. R. Holstein, Dynamics of the standard model, Cambridge Monogr. Part. Phys., Nucl. Phys., Cosmol. **2**, 1 (1992); **35**, 1 (2014).
[154] M. Ademollo and R. Gatto, Nonrenormalization Theorem for the Strangeness Violating Vector Currents, Phys. Rev. Lett. **13**, 264 (1964).
[155] H. Leutwyler and M. Roos, Determination of the elements V(us) and V(ud) of the Kobayashi-Maskawa matrix, Z. Phys. C **25**, 91 (1984).
[156] R. F. Lebed and M. Suzuki, Current algebra and the Ademollo-Gatto theorem in spin flavor symmetry of heavy quarks, Phys. Rev. D **44**, 829 (1991).
[157] T. Yamazaki, Search for Exotics in two-body decay of $K+$: K(mu2) and K(pi2) revisited, *Proceedings of the Second LAMPF II Workshop* (Los Alamos National Laboratory, Los Alamo, 1982), Vol. II, p. 413.
[158] T. Yamazaki *et al.*, Search for a Neutral Boson in a Two-Body Decay of $K+ >$ pi+$X0$, Phys. Rev. Lett. **52**, 1089 (1984).
[159] N. J. Baker *et al.*, Search for Shortlived Neutral Particles Emitted in K^+ Decay, Phys. Rev. Lett. **59**, 2832 (1987).
[160] J. R. Batley *et al.* (NA48/1 Collaboration), Observation of the rare decay $K(S) \to$ pi0 e + e−, Phys. Lett. B **576**, 43 (2003).
[161] G. D. Barr *et al.* (NA31 Collaboration), Search for the decay $K(S) \to$ pi0 e + e−. CERN-NA031 experiment, Phys. Lett. B **304**, 381 (1993).
[162] A. Lai *et al.* (NA48 Collaboration), Search for the decay $K(S) \to$ pi0 e + e−, Phys. Lett. B **514**, 253 (2001).
[163] G. D. Barr *et al.* (NA31 Collaboration), Search for a neutral Higgs particle in the decay sequence $K0(L) \to$ pi0 H0 and $H0 \to$ e + e−, Phys. Lett. B **235**, 356 (1990).
[164] J. Adams *et al.* (KTeV Collaboration), Measurement of the Branching Fraction of the Decay $K(L) \to$ pi + pi − e + e−, Phys. Rev. Lett. **80**, 4123 (1998).
[165] Y. Takeuchi *et al.*, Observation of the decay mode $K(L) \to$ pi + pi − e + e−, Phys. Lett. B **443**, 409 (1998).
[166] A. Lai *et al.* (NA48 Collaboration), Investigation of $K(L, S) \to$ pi + pi − e + e− decays, Eur. Phys. J. C **30**, 33 (2003).
[167] D. Ambrose *et al.* (BNL E871 Collaboration), First Observation of the Rare Decay Mode $K0(L) \to$ e + e−, Phys. Rev. Lett. **81**, 4309 (1998).
[168] L. M. Sehgal, Electromagnetic contribution to the decays $K(S) \to$ lepton anti-lepton and $K(L) \to$ lepton anti-lepton, Phys. Rev. **183**, 1511 (1969); Erratum, Phys. Rev. D **4**, 1582 (1971).
[169] G. Valencia, Long distance contribution to $K(L) \to$ lepton+ lepton−, Nucl. Phys. **B517**, 339 (1998).
[170] D. G. Dumm and A. Pich, Long Distance Contributions to the $K(L) \to u +$ mu− Decay Width, Phys. Rev. Lett. **80**, 4633 (1998).

Correction: The terms in Eq. (78) were improperly misaligned during the final production stage and have been fixed.